CINTAL - Centro de Investigação Tecnológica do Algarve

Universidade do Algarve

INTIFANTE'00 Sea Trial

Data Report - Events I,II and III

S.M. Jesus, A. Silva and C. Soares

Rep 02/01 - SiPLAB
4/May/2001

University of Algarve
Campus da Penha
8000, Faro,
Portugal

tel: +351-289800131
fax: +351-289864258
cintal@ualg.pt
www.ualg.pt/cintal

Work requested by	CINTAL Universidade do Algarve, Campus da Penha, 8000 Faro, Portugal tel: +351-289800131, cintal@ualg.pt, www.ualg.pt/cintal
Laboratory performing the work	SiPLAB - Signal Processing Laboratory Universidade do Algarve, FCT, Campus de Gambelas, 8000 Faro, Portugal tel: +351-289800949, info@siplab.uceh.ualg.pt, www.ualg.pt/uceh/adeec/siplab
Projects	INTIMATE - FCT, 2/2.1/MAR/1698/95 INFANTE - FCT, 2/2.1/TPAR/2042/95 ATOMS - FCT, PDCTM/P/MAR/15296/1999
Title	INTIFANTE'00 Sea Trial - Data Report, Events I,II,III
Authors	S.M.Jesus, A.Silva and C.Soares
Date	May 4, 2001
Reference	02/01 - SiPLAB
Number of pages	53 (fifty three)
Abstract	This report describes the data acquired during Events I, II and III of the INTIFANTE'00 sea trial, that took place from 9 - 29 October 2000, off the Tróia Peninsula, near Setúbal, Portugal.
Clearance level	UNCLASSIFIED
Distribution list	DUNE (1), ENEA (1), IH (1), IST (1), SACLANTCEN (1), SiPLAB (1), CINTAL (2)
Total number of copies	8 (eight)

Foreword and Acknowledgment

This report presents the real data acquired during Events I, II and III of the INTIFANTE'00 sea trial. The INTIFANTE'00 sea trial took place off the Tróia Peninsula, near Setúbal, approximately 50 km south of Lisbon, Portugal, during the period 9 - 29 October 2000.

The institutions responsible for the sea trial are:

- Instituto Hidrográfico, Rua das Trinas 49, Lisboa, Portugal.
- CINTAL, Universidade do Algarve, Faro, Portugal.
- ISR, Instituto Superior Técnico, Lisboa, Portugal.

Other institutions involved are:

- Ente Nazionale per l'Energia ed l'Ambiente, La Spezia, Itália

The INTIFANTE organizers would like to thank:

- the crew of the research vessel NRP D. Carlos I
- the NATO SACLANT Undersea Research Centre for lending the acoustic sound source and power amplifier.
- Enrico Muzi, from SACLANTCEN, for his participation in the acoustic source preparation and testing.
- the collaboration of ADEE, Escola Superior de Tecnologia (EST) of Universidade do Algarve in the preparation of Event 1.

intentionally blank

Contents

List of Figures

Chapter 1

Introduction

Sound propagation in the ocean is highly dependent on the environmental characteristics of the propagation media between the source and the receiver. Since the oceanic environment is continuously changing in time and space, using acoustics for underwater communication and sonar detection are very challenging tasks. Conversely, the interaction between sound waves and the environment allows for retrieving environmental information from the analysis of the emitted and received signals - this is known as acoustic tomography[1], [2]. Therefore, being able to predict the acoustic behaviour of a given environment is the key to current advances in the usage of underwater acoustics for ocean exploration.

In 1997, the Portuguese Foundation for Science and Technology (FCT)[1] has founded two initiatives in marine technology, namely projects INTIMATE[2] and INFANTE[3]. The former aims at developing and testing ocean tomography techniques for estimating internal tides in the continental platform. The later aims at developing autonomous underwater vehicles (AUVs) and includes a component of testing methods and algorithms for improving the capabilities of the underwater communication channel between the surface and a submerged vehicle.

The INTIFANTE'00[4] sea trial was carried out in the vicinity of Setúbal, situated approximately 50 km to the south of Lisbon, in Portugal, during the period from 9 to 29 October, 2000. The leading institutions were the Instituto Hidrográfico, that carried out the oceanographic observations and managed the research vessel NRP D. Carlos I, CINTAL/UALG that provided the acoustic data acquisition system and the emitted source signal control and IST, that was in charge of the high frequency data communications testing. Other collaborating/participating institutions were the NATO SACLANT Undersea Research Centre with the loan of the acoustic sound source and respective power amplifier and the Ente Nazionale per l'Energia ed l'Ambiente (ENEA) that participated in the hydrological survey.

This sea trial served a number of specific purposes under the leading projects INTIMATE and INFANTE, namely to acquire data for testing the Time-Reversal Mirror (TRM) for underwater communications at low-frequency (Event 1), internal tide acoustic tomography through a 25 hours observation of continous transmissions (Event 2), source

[1]Fundação para a Ciência e a Tecnologia, Ministry of Science and Technology
[2]"Internal Tide Measurements with Acoustic TOmography Experiments"
[3]"Development of Vehicles and Advanced Systems for Submarine Inspection"
[4]INTIFANTE is a madeup acronym from INTImate and inFANTE.

localization and tracking over strong environmental variability, (Event 3) and over a mild range dependent environment (Event 4). The data sets acquired during Events 1 to 3 are described in this report while Event 4 is described in a companion report[3]. The experiment area was a rectangular box situated in the border of the continental platform with depths varying from 60 to 140 m and including a sharp submarine canyon (the Setúbal canyon) with depths rapidly reaching over 500 m. As an overview of the technical aspects involved in the experiment, it can be referred that acoustic signals were transmitted with an acoustic projector from onboard NRP D. Carlos I and received on a moored 16 hydrophone-4m spacing Vertical Line Array (VLA). The acoustic aperture of the vertical array was located between 30 and 90 m in a 120 m water column. The acoustic signals received in the VLA were transmitted via an RF link to the research ship NRP D. Carlos I, processed, monitored and stored. Various signals were emitted by the sound projector ranging from linear frequency modulated (LFM) sweeps, to broadband MPSK modulated binary sequences .

This report is organized as follows: section 2 gives an overview of the INTIFANTE'00 sea trial. Section 3 deals with the description of the environmental data, such as bathymetry, bottom properties and hydrological information. Section 4 describes the overall geometry of the experiment like ship's position and source - receiver geometry and finally section 5 describes the acoustic data gathered at the VLA. Some conclusions are drawn in section 6.

Chapter 2

The INTIFANTE’00 sea trial

2.1 Generalities and sea trial area

The INTIFANTE’00 experiment was carried out in the period from 9 - 29 October 2000, off the town of Setúbal, 50 km south from Lisbon, Portugal. The research vessel NRP D. Carlos I, managed by IH, was in charge of deploying all equipment, sending and receiving all signals to/from vertical array and making the necessary environmental surveys. The experimental scenario is depicted in figure 2.1.

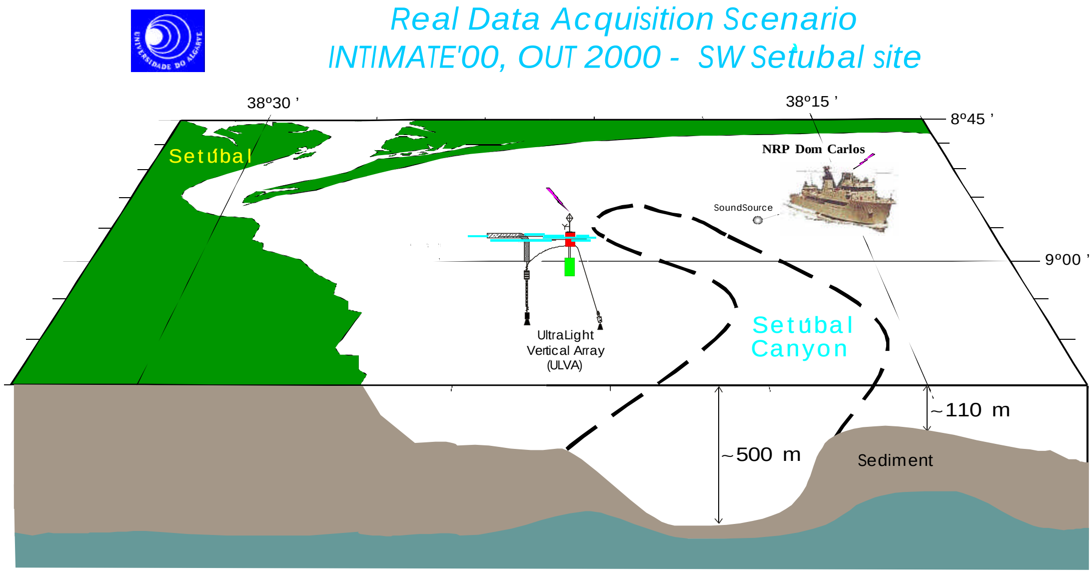

Figure 2.1: *INTIFANTE’00 experimental scenario*

The acoustic receiver was a 16-hydrophone 4-m spacing VLA suspended from the sea surface by a free floating rubber hose for wave action decoupling (see figure 2.2). The array also had a number of non-acoustic sensors such as 8 thermistors, 2 tiltmeters and

2 pressure gauges. All signals received at the array were sampled and multiplexed in a telemetry unit, cabled to the surface buoy to be transmitted via an high speed data link to the NRP D. Carlos I. On board ship, the signals were demultiplexed, monitored and saved to disk together with GPS time synchronization marks allowing for absolute time datation. The NRP D. Carlos I was also transmitting acoustic signals with a sound projector imerged at variable depths, depending whether on station or under tow. Emitted signals were computer generated and then transmitted to the power amplifier at specified times synchronous with GPS, and therefore also synchronous to the received signal datation scheme.

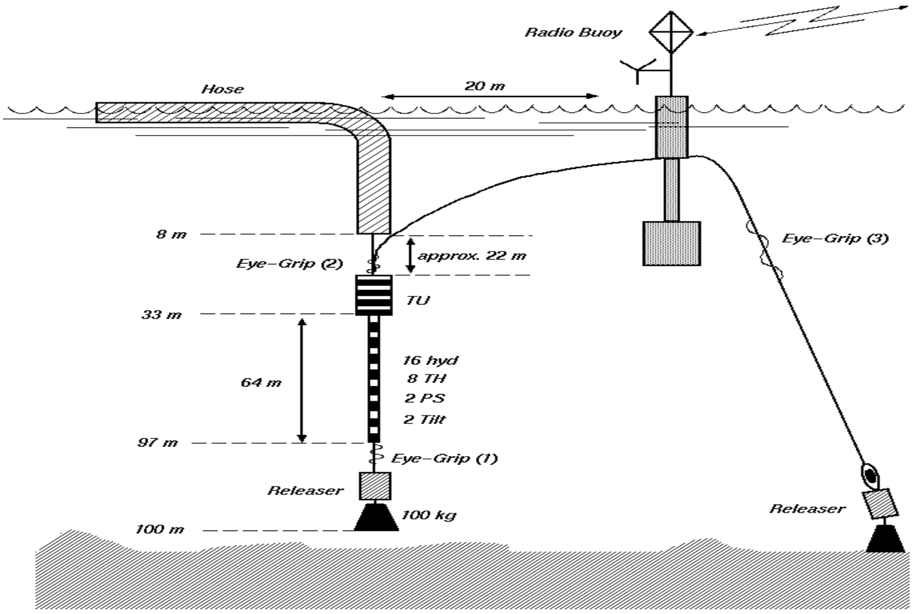

Figure 2.2: *Vertical Line Array(VLA) structure.*

Ship movements were performed within a specified sea trial area. The bounding box reserved for the sea trial is shown in figure 2.3 with the coordinates shown in 2.1.

Table 2.1: *Experimental site bounding box*

9°	3'	0"	W,	38°	22'	0"	N
8°	50'	0"	W,	38°	22'	0"	N
9°	3'	0"	W,	38°	13'	0"	N
8°	50'	0"	W,	38°	13'	0"	N

The choice of this area was made based on a number of factors among which that it is naturally protected from North winds by the Espichel Cape (North - West from site) and guarantees stable conditions for the development of work at sea. This is a relatively well known area from the oceanographic, hydrological and geophysical points of view as it has been previously explored by IH [5], [6]. The area itself is a portion of the continental platform with various bathymetric characteristics as shown in the detailed figure 2.4. The area is extending to shore in its eastern side attaining depths of only 40 m, to northwest in a relatively range independent plateau at 120 m depth, to the southwest nearly at the shelf edge at 200 m depth. The area is crossed from west to east by the Setúbal Canyon that reaches depths as low as 800 m and extending into the continental plateau for about 20 miles. As can be seen in the sediment structure shown in figure 2.4, the bottom of the area is predominantly covered by sand and mud with a few localized rock patches.

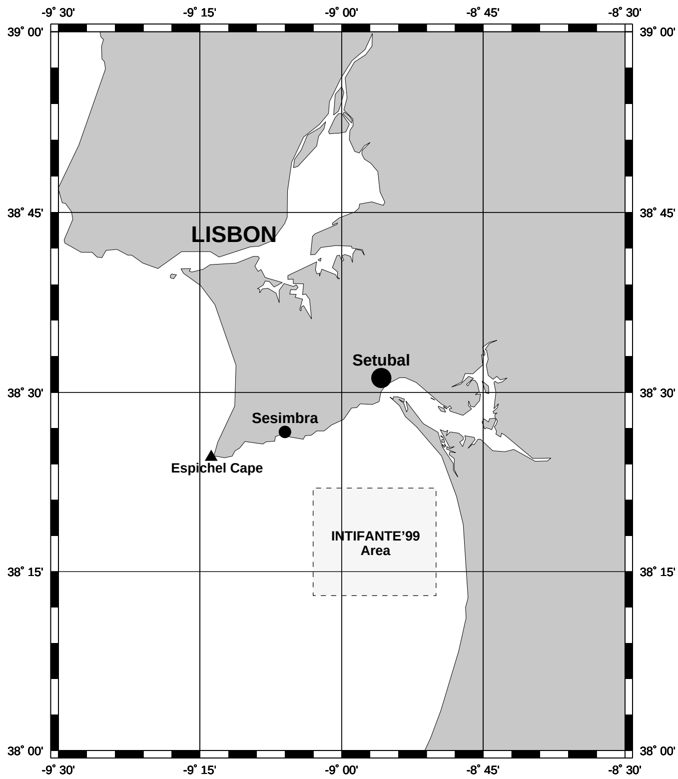

Figure 2.3: *Localization of the experimental site*

The bottom type is largely invariant in the plateau zone and the Canyon, while strongly variant when approaching shore.

The three black lines in figure 2.4 represent the acoustic transmission legs, while the crossing point is the VLA location; T2, T4 and T5 denote the locations of the currentmeter line moorings used during this sea trial. Figure 2.4 depicts the experimental area and sea trial geometry as planned prior to the experiment itself. Actual mooring locations are given in an IH companion report and ship movements are given in the next chapters.

2.2 List and description of Events

The full list of Events planned for the INTIFANTE'00 sea trial is detailed in the Test Plan [4]. The Events of concern for INFANTE and INTIMATE projects are numbers 1, 2, 3 and 4 conducted during days 16 - 19 of October as referred to in table 2.2.

Event 4 is described in a companion report[3] prepared for TOMPACO project, so it will not be repeated here. Events 1,2 and 3 listed in table 2.2 were performed along the northwest and southeast transmission legs or nearby the VA so we will concentrate in those areas in the sequel. The data shown in this report has been archived in a series of CD-ROMS (see list in appendix A) for posterior distribution among the participating teams in agreement with the data distribution rules setforth in the INTIFANTE'00 testplan.

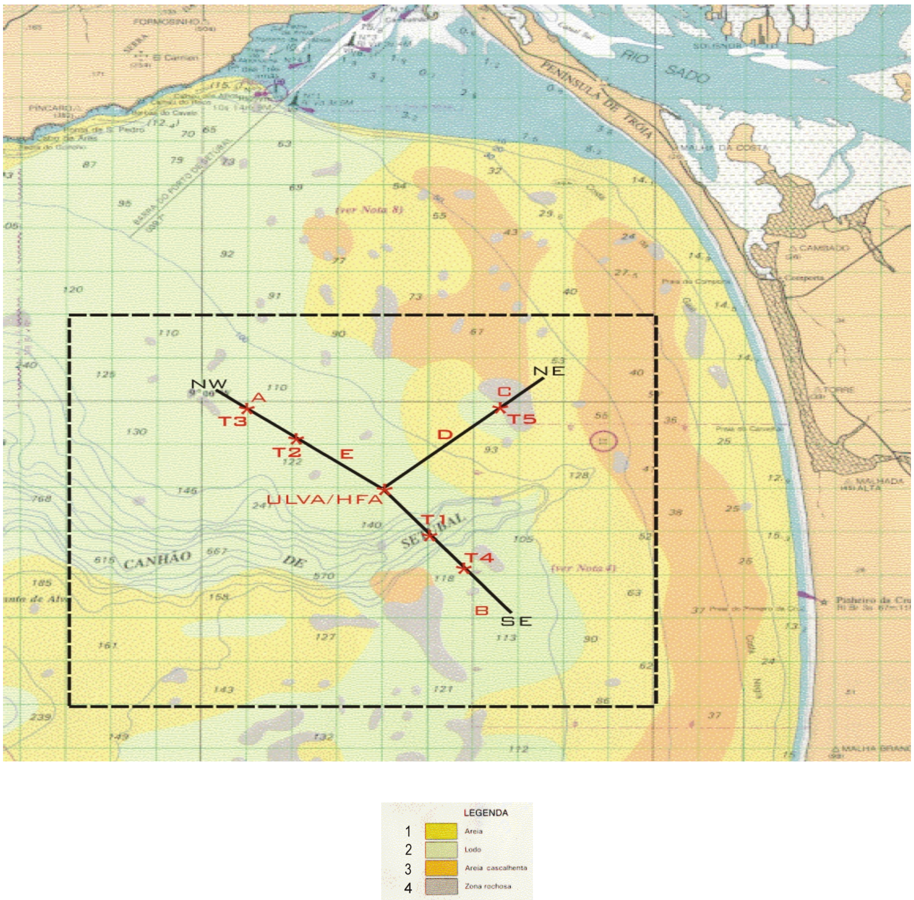

(1)Sand, (2)Mud, (3)Sand and gravel, (4)Rock.

Figure 2.4: *Bathymetry and bottom structure*

Table 2.2: *INTIFANTE Event list*

Event	**Start** date-time(UTC)	**End** date-time(UTC)	**Code**	**Description**
Ev1	16/10-01:00	16/10-09:00	D	MPSK modulated sequences
Ev2	17/10-14:30	18/10-13:00	A3	transmitted LFM sweeps
Ev3	18/10-03:30	19/10-04:00	A3	transmitted LFM sweeps
Ev4	17/10-19:00	18/10-22:30	A3	transmitted LFM sweeps

Chapter 3

Environmental data

This section deals with the description of all non-acoustic site specific information gathered during the sea trial like bathymetry, bottom properties and water column temperature measurements.

3.1 Bottom properties and bathymetry

3.1.1 Site bathymetry

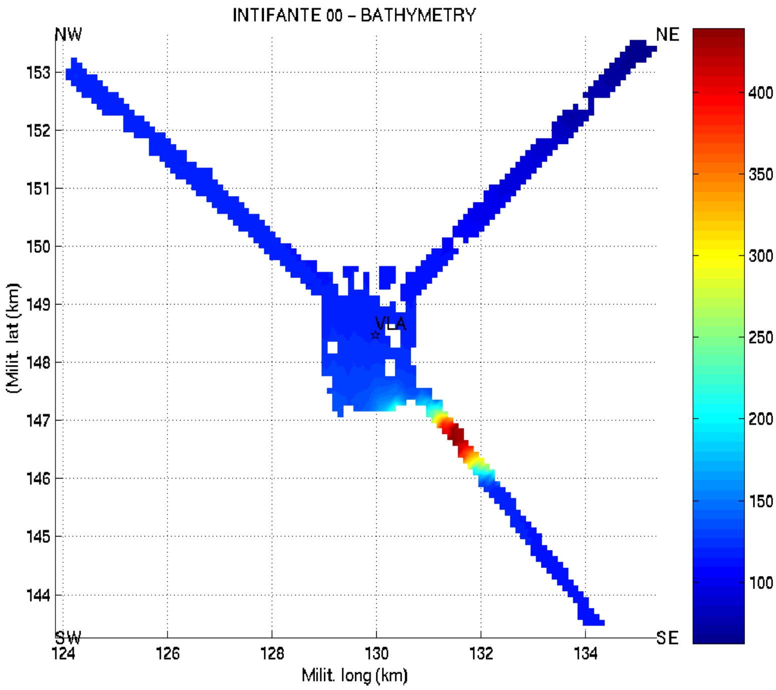

Figure 3.1: *Site bathymetry along the acoustic transmission tracks (depth in m). VLA location is denoted by* $\star$.

The sea trial area bathymetry was extensively surveyed by NRP D. Carlos I during the week 23 - 29 October. A partial bathymetry map along the acoustic transmission tracks is given in figure 3.1. The full survey will be available in the IH companion report.

3.1.2 Sediment characteristics

The acoustic transmission tracks have been surveyed during the INTIFANTE'99 with both a sidescan sonar and a light seismic Sparker system. During INTIFANTE'00 a second sidescan sonar survey was performed in the last sea trial week and will be included in a companion IH report.

3.2 Hydrological data

Hydrological data encompasses XBT and thermistor recordings. XBT casts were performed by ENEA from onboard D. Carlos I at various times. Thermistor recordings were made at the VLA location by the built in sensors.

3.2.1 XBT data

XBT casts were made approximately every 3 hours with the objective of capturing the tidal evolution. Figure 3.2 shows 14 XBT recordings (a) and the respective calculated sound velocity profiles (b). The displacement that can be seen in the first 4 calculated sound velocity profiles is due to an erroneous salinity setting during the cast itself. A strong downward refracting gradient can be seen at an approximate depth of 10 m to over 50 m. The oscillation of the termocline along time can be seen in figure 3.3, where, even if largely undersampled, a semi-diurnal tidal effect can be clearly seen.

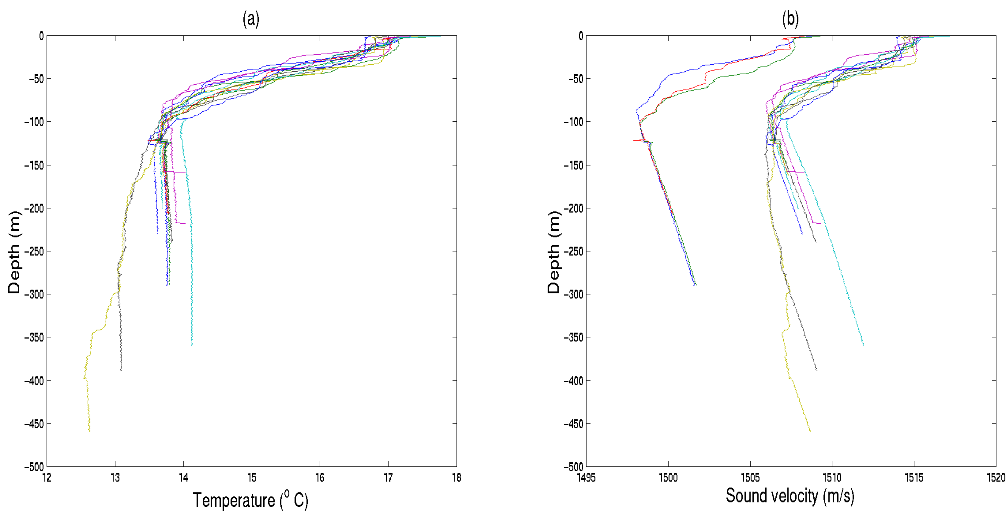

Figure 3.2: *XBT data: temperature (a) and calculted sound velocity (b).*

From a spatial point of view XBT casts were made from NRP D. Carlos I and therefore always at the source location while the ship was moving along the various tracks perform-

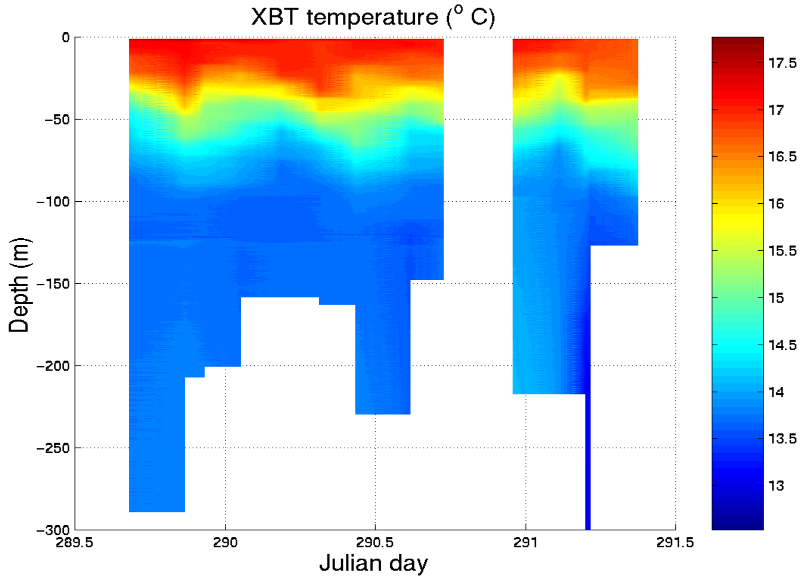

Figure 3.3: *Recorded XBT temperature variation through time.*

ing acoustic transmissions. Figure 3.4 shows the positions of all XBT's in the sea trial area together with the fast track bathymetry and the VLA position.

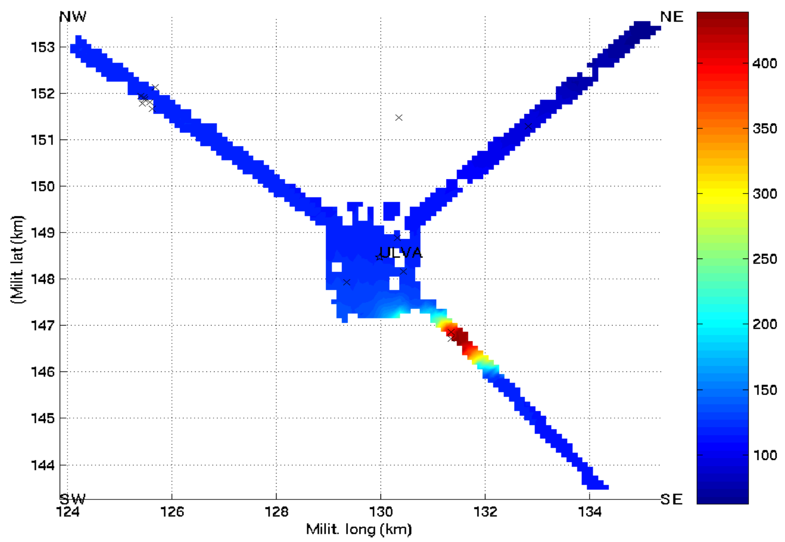

Figure 3.4: *Location of XBT casts denoted by the* $\times$ *positions.*

3.2.2 Thermistor data

Temperature data was gathered from the thermistor sensors colocated with the VLA. While the XBT casts were supposed to capture the semi-diurnal behaviour of the tidal flux and a high-resolution spatial variation of the temperature field in the water column, the thermistor sensors were intended to obtain a high temporal resolution at selected depths and at a fixed location. The VLA has 8 temperature sensors with a 8 m spacing.

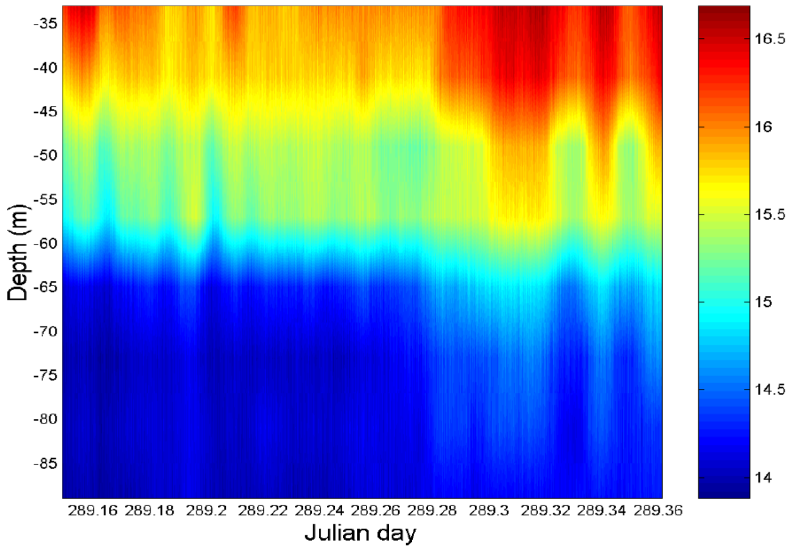

Figure 3.5: *Temperature field recorded at the VLA during Event 1.*

The first sensor is located 3 m below the shallowest pressure gauge that was recording a mean depth of 30 m. So, temperature was recorded at approximate depths of 33, 41, 49, 57, 65, 73, 81 and 89 m, depending on the precision of the pressure gauge sensor and tilt of the vertical array.

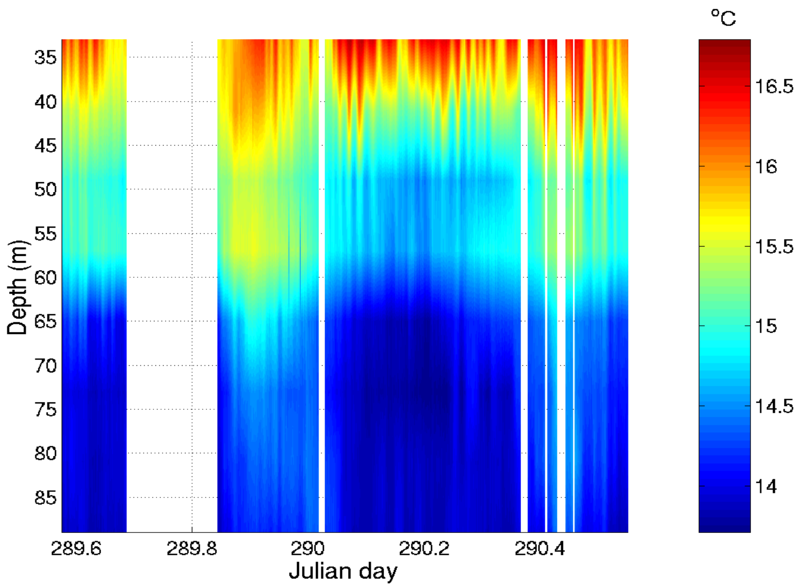

Figure 3.6: *Temperature field recorded at the VLA during Event 2.*

The temperature field is shown in figures 3.5 to 3.7 for Events 1, 2 and 3 respectively. Event 1 lasted for approximately 4 hours and 20 minutes with a 20 minute interruption. Event 2 started at approximately 14:48 GMT and suffered a long interruption for changing VLA batteries before sunset (figure 3.6). Than there is a long period of almost 20 hours of continuous transmission, with a few short interruptions due to the changing of recording media. The oscillation of the thermocline can be detected with, however, a not so clear change of temperature ranges from section to section. The evolution of temperature as measured at the VLA location during Event 3 is shown in figure 3.7. Also in this case there is along interruption of a few hours and a clear oscillation during the second portion of the recording.

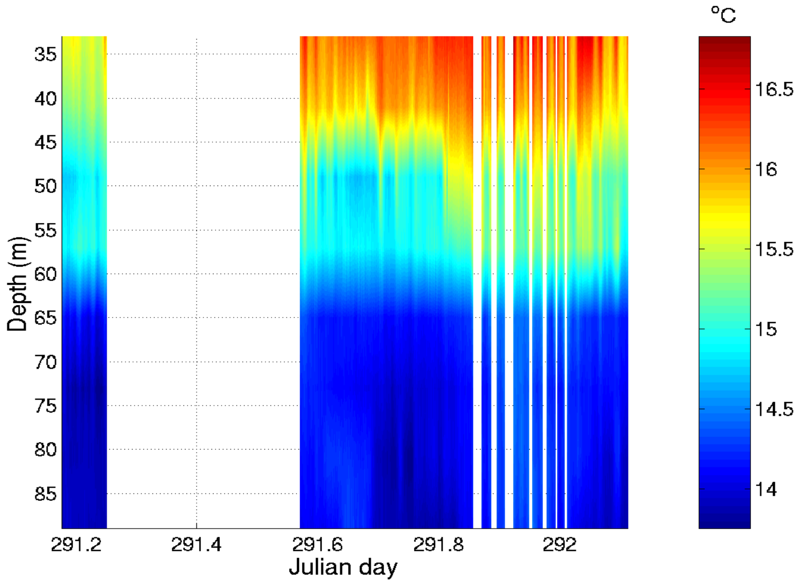

Figure 3.7: *Temperature field recorded at the VLA during Event 3.*

Chapter 4

Experiment geometry

This section describes the ship's position as logged from GPS during the experiment. The relative position between source and receiver is deduced from the known VLA mooring position and the ship GPS log. The position of the VLA elements is estimated from the depth sensor and tilt recordings. Source depth is deduced from the source colocated depth sensor recordings and cable scope.

4.1 Ship position

Ship position was permanently recorded through the onboard GPS navigation system and by a parallel GPS system connected to the data recording station. In order to avoid confusion between several parallel tracks from different systems only the data provided by the data recording station GPS is used. Figures 4.1 to 4.6 show all the ship's positioning data for Events 1,2 and 3.

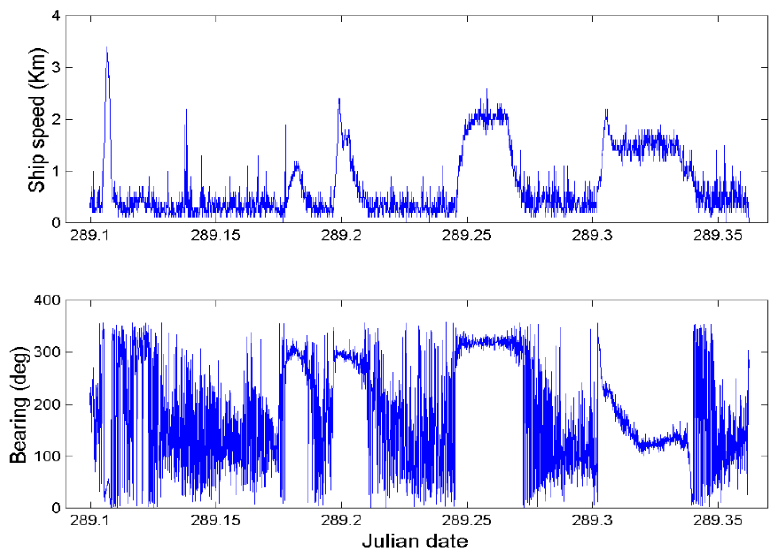

Figure 4.1: *Event 1: ship speed (a) and ship's heading (b).*

4.1.1 Event 1: time-reversal mirror testing

During Event 1, NRP D. Carlos I was supposed to start transmissions close by the VLA and then steam to location C along the NW leg making stations as requested. Maximum range of last station was to be determined during the experiment. The GPS data is shown in figures 4.1 for ship's speed (a) and heading (b) and in figure 4.2 for ship's course along time. During the first part of the Event, and acording to figure 4.2, the ship was drifting by the VLA. After aproximately time 289.155, the ship took course by 300 degrees, which roughly corresponds to the orientation of leg A, at an approximate constant speed of 1 kn. That course was interrupted after a short while and then resumed at a faster speed of 2 kn and then interrupted again for a longer period between 289.21 and 289.25. The same course was resumed again until reaching the last station that was kept for about 1 hour. In the way back to the VLA ship speed was about 1.5 kn and course was 100 degrees stopping for a last station at 289.34 (see figure 4.2).

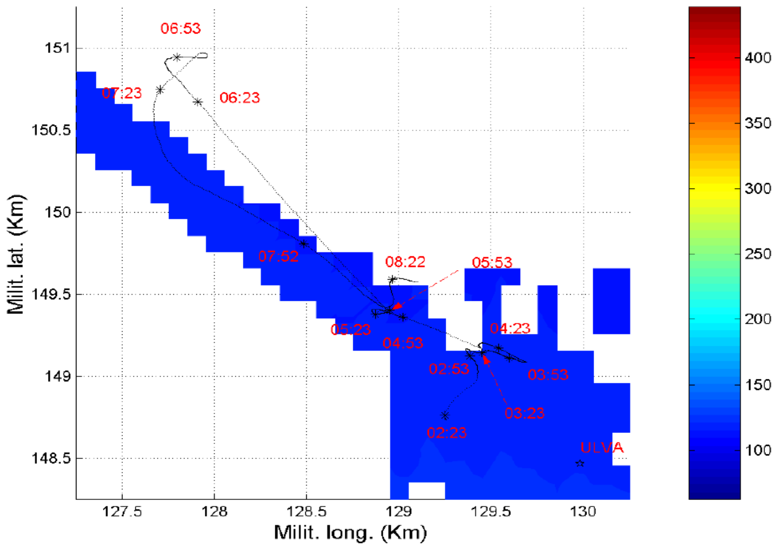

Figure 4.2: *Ship course during Event 1.*

4.1.2 Event 2: range independent acoustic transmissions

This Event started with the ship at the VLA location and then steaming to location A, along the NW leg. The GPS data is shown in figures 4.3 for ship's speed (a) and heading (b) and in figure 4.4 for ship's course along time. It clearly shows a constant ship heading of 300 degrees at 1.2 kn in the first portion of the plot of figure 4.3. In the second portion of the same figure the ship kept the position at very low speed. In the end of the Event the ship steamed back to the VLA at nearly 3 kn with heading 120 degrees. That information is consistent with the ship track shown in figure 4.4.

4.1.3 Event 3: across canyon acoustic transmissions

During Event 3 the recording started nearby the VLA and continued while the ship was moving to 120 degrees at 1.5 kn towards location B (figure 4.5), crossing Setúbal submarine

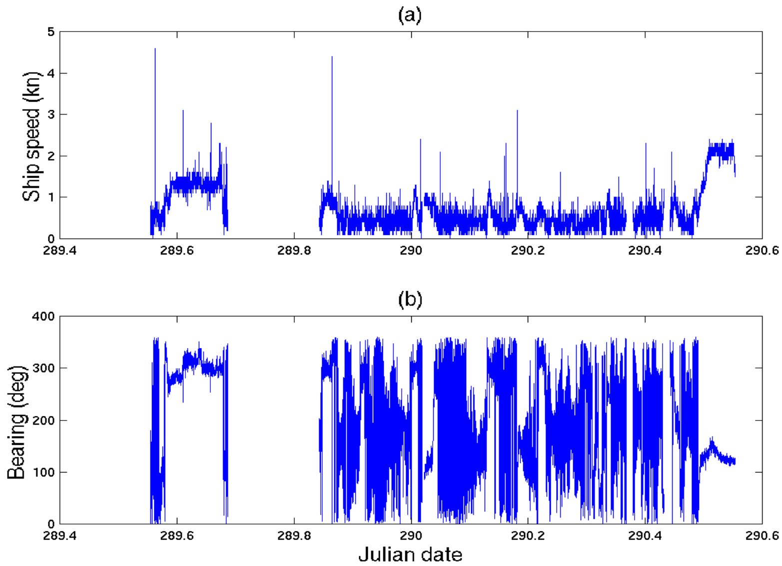

Figure 4.3: *Event 2: ship speed (a) and ship's heading (b).*

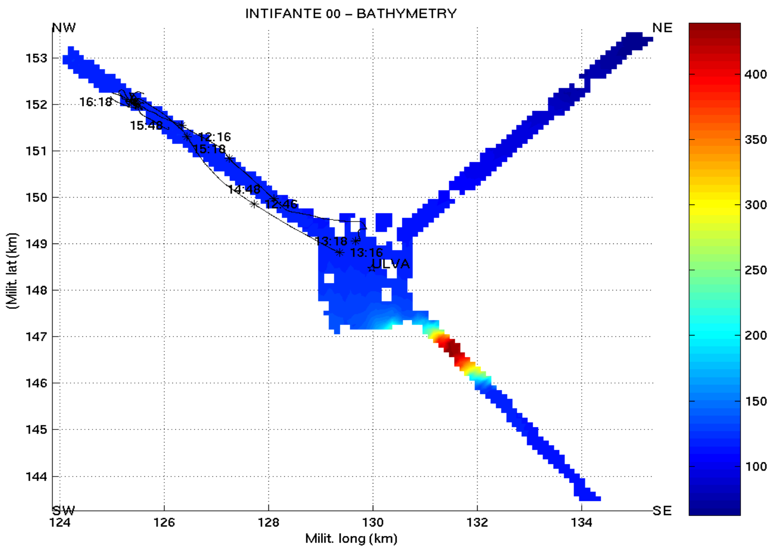

Figure 4.4: *Ship course during Event 2.*

canyon, as shown in the bathymetry map of figure 4.6. After the interruption, acoustic transmissions have resumed at location B until the end of the Event.

4.2 Source depth

The pressure gauge inserted in the acoustic source failed to work due to a driving cable malfunction during the testing phase. An alternative self-recording pressure gauge was attached to the acoustic source tow cable at approximatelly 1.5 m from the source. The tow cable was also tickmarked every 5 m. After a given moment that depth sensor was

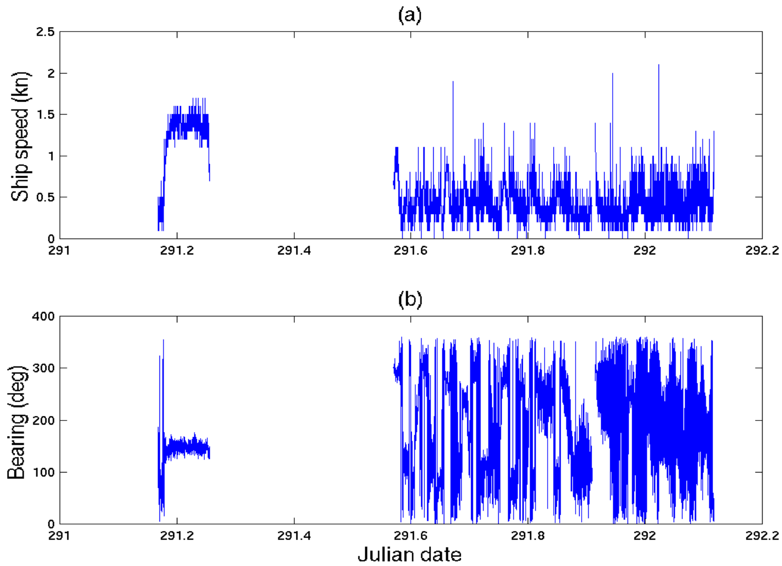

Figure 4.5: *Event 3: ship speed (a) and ship's heading (b).*

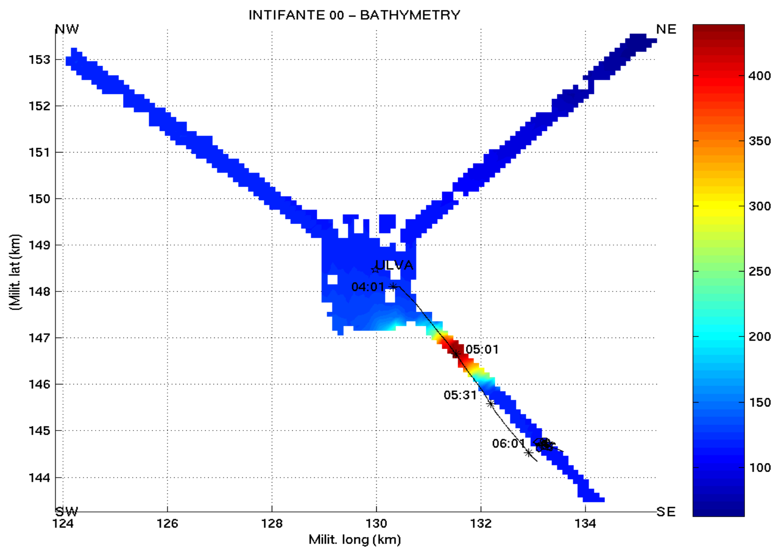

Figure 4.6: *Ship course during Event 3.*

also broken. From that moment on we were reduced to work with the paycable vs. depth calibration figures given by SACLANTCEN for that source and tow cable as reproduced in figure 4.7. Source cable scope during the three Events 1,2 and 3 is given in table 4.1. This information is to be completed with IH recordings obtained from the depth sensor directly located on the source during the period it was working.

Table 4.1: *Acoustic source cable scope.*

Event	**Start** date-time(UTC)	**End** date-time(UTC)	**Cable scope** (m)
Ev1	16/10-03:00	16/10-09:00	66
Ev2	16/10-13:50	17/10-13:15	66
Ev3	18/10-13:40	19/10-02:50	47

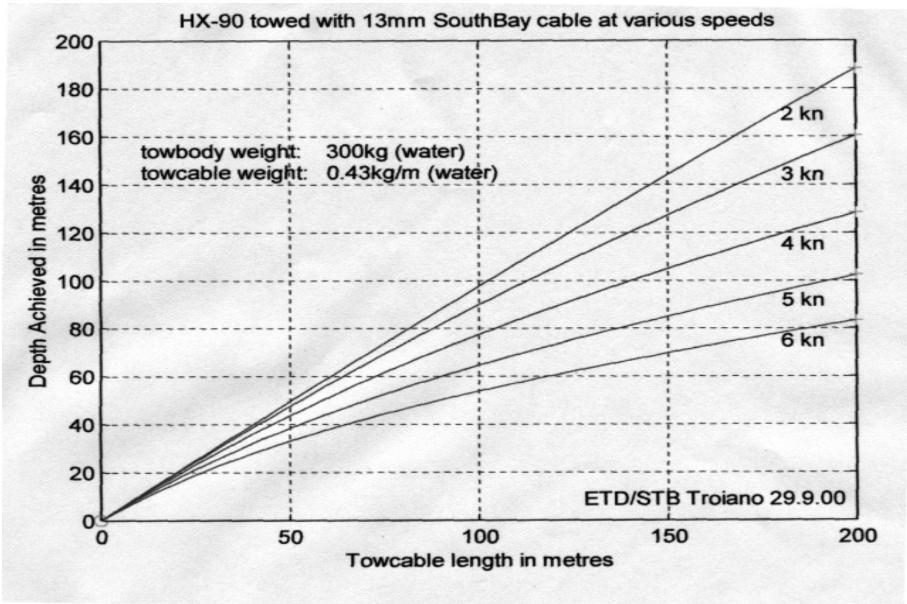

Figure 4.7: *HX90 source depth as a function of cable length for various ship speeds.*

4.3 Receiver depth and tilt

The VLA was equiped with two pressure gauges and two X-Y tiltmeters. The recordings of depth and tilt sensors are shown in figures 4.8 to 4.10 for Events 1, 2 and 3 respectively. During Event 1 both the shallowest and deepest depth sensors are relatively stable through time around 30.5 and 92.5 m depth respectively(figure 4.8(a) and (b)). The distance of 62 m between th two depth sensors is consistent with the physical length of the array, denoting however a possible small array tilt. Plots (c) and (d) of figure 4.8 represent the top and bottom tilt sensors along the X axis(green) and Y axis(blue). These curves are much more difficult to interpret since the orientation of the X and Y axis are not referred to an absolute direction. The only conclusions that may be drawn from these curves is that 1) the array is nearly vertical in the top portion with a mean tilt around 0 degrees both in the X and Y axis with a large standard deviation of about 5 degrees, what may be due to sea surface agitation, 2) the array has a pronounced tilt in the bottom portion with an X and Y axis mean value of 4 and -2 degrees respectively, and 3) there is an increasing array movement by the end of the Event (around 289.3) only in the bottom X-Y sensors.

The pressure gauges and tilt sensors recordings made during Event 2 are shown in figure 4.9 (a)-(b) and (c)-(d) respectively. Mean values of top and bottom depth sensors are similar to those obtained during Event 1 with, however, a larger amplitude of oscillations and also slightly larger than during Event 3. In particular a clear oscillation can be noticed in the second portion of the recording; curiously that oscillation seems to be in phase with

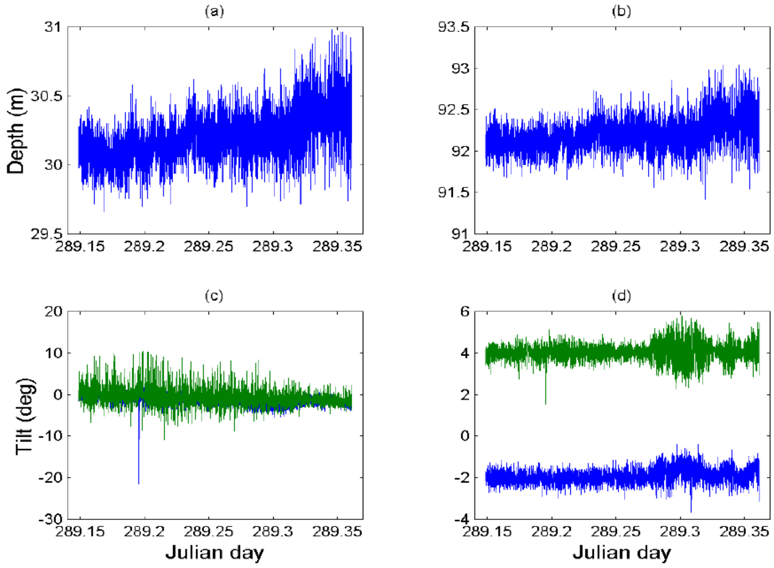

Figure 4.8: *Event 1: receiving array depth (a)-(b) and tilt (c)-(d).*

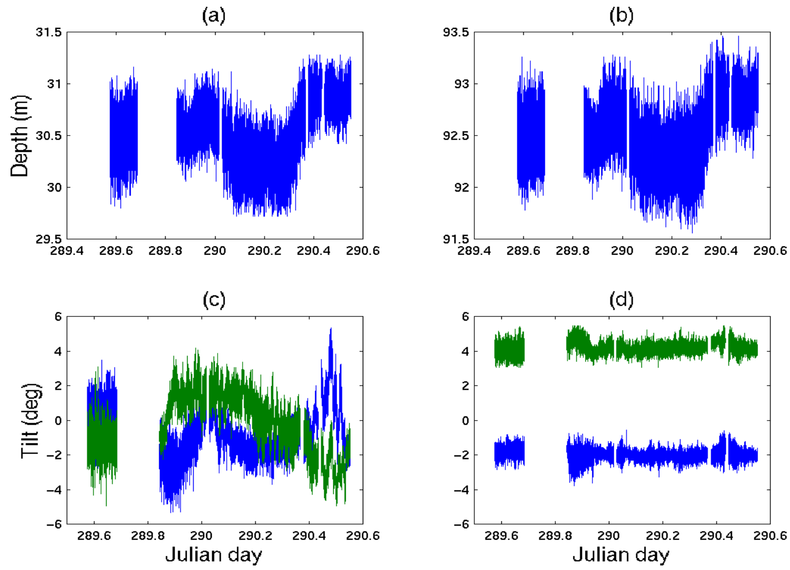

Figure 4.9: *Event 2: receiving array depth (a)-(b) and tilt (c)-(d).*

the oscillation seen in the temperature recordings made at the VLA for the same Event (figure 3.6). Regarding the tiltmeter recordings, they are remarkably consistent with those obtained for the bottom sensors during Event 1. The top sensors show a strange pattern of inversion of tilt between X and Y axis during the second portion of the run (exactly coincident with the oscillation mentioned above for the depth sensors) denoting, possibly, an inversion of tilt at a change of tidal cycle.

Figure 4.10 shows the recording of depth and tilt made during Event 3. Depth recording has mean values consistent with those recorded previously with however a remarkable correlation between the top and bottom sensors throughout the run. The tilt sensors show some variability for the top sensor in coincidence with the pressure recording and a stable pattern for the bottom recordings when compared to previous Events.

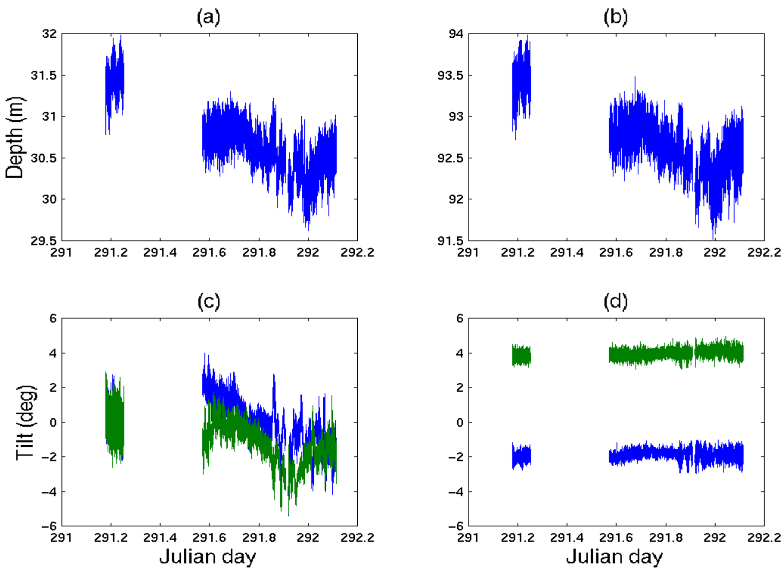

Figure 4.10: *Event 3: receiving array depth (a)-(b) and tilt (c)-(d).*

Chapter 5

Acoustic data

5.1 Transmitted signals

The signals being transmitted with the acoustic sound source were computer generated time sequences with specific characteristics. A complete list of signals available for the sea trial is in appendix A of [4]. The codes used during Event 1 are a series of Phase Shift Keying (PSK) modulated binary sequences at various rates and frequency bands. A full list of the transmitted codes used in Event 1 is given in appendix B. The codes in that list can be divided in test codes and data codes. Test codes are used for testing purposed only, and do not contain data, while data codes contain a known binary sequence as valid data being transmitted. Both test codes and data codes are formed by a preliminary signal - called probe signal - and a data packet.

5.1.1 Event 1: probe signal

The probe signal acts like an header of the message itself and has always a fixed duration of 1 second. The shape of the probe signal is the pulse shape of the PSK modulation, which mainlobe duration depends on the symbol rate: the higher the symbol rate the shorter the mainlobe. The pulse shape itself is a root-root raised cosine with 50% roloff as shown in figure 5.1(a) with the pulse spectrum shown in 5.1(b) for symbol rates 75, 150 and 300 symb./s.

5.1.2 Event 1: test codes

Test codes are used as test signals and can be divided in two types: the 'te' and the 'lf' types. The 'te' type has the same structure as the data codes, i.e.,they contain a probe signal and a PSK modulated data packet. The probe signal has the structure described above for the 75 symb./s pulse shape. The data packet is a PSK2 modulated sequence of a repetition of symbol '1'. Instead, the 'lf' type is formed by a series of probe signals followed by a series of LFM upsweeps without any type of modulation. The LFM sweeps have a duration of 0.5 s and a band between 1.2 and 2 kHz. There are two possible 'lf' test codes: the N5PSK2lf, that has 3 s of probe signals followed by 3 s of LFM's and the N20PSK2lf, that has 10 s of probe signals followed by 10 s of LFM's. Test codes

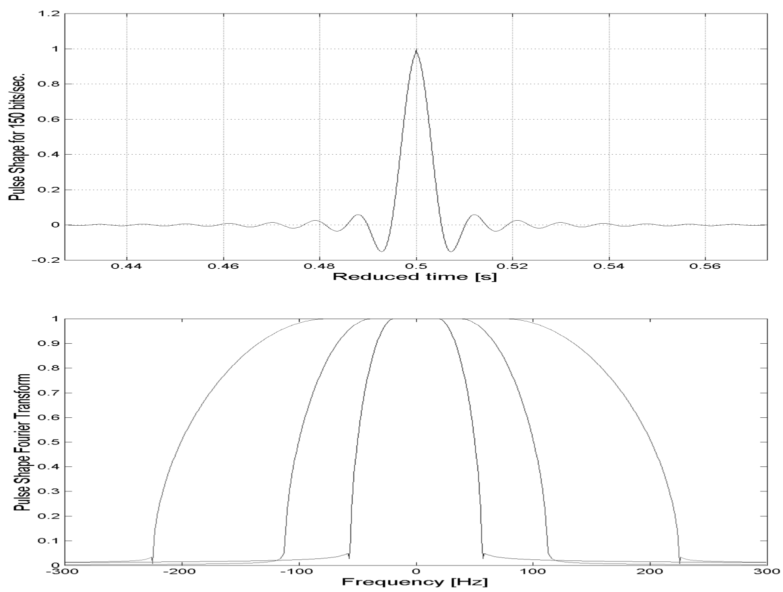

Figure 5.1: *Root-root raised cosine pulse shape (a) and its spectrum for 75, 150 and 300 symbols/s(b).*

parameters are shortly described in table 5.1.

Table 5.1: *Event 1: test code parameters.*

Code	**Probe**		**Data**		**Duration**	**Rep.rate**
	type	duration (s)	modulation	data	(s)	(s)
N20PSK2te	PS75	1	PSK2	bit"1"	20	22
N5PSK2te	PS75	1	PSK2	bit"1"	5	7
N20PSK2lf	PS75	10	LFM	-	10	22
N5PSK2lf	PS75	3	LFM	-	3	7

5.1.3 Event 1: data codes

Data codes are formed by a probe signal (PS) followed by a PSK modulated binary data sequence(DS). The binary DS is a stream of 0's and 1's with duration of 5 or 20 seconds at different symbol rates of 75, 150 or 300 symb/s. The DS is formed as a random sequence of symbols that is different for each code. PSK modulations used are binary (PSK2), quadrature (PSK4) and octal (PSK8), therefore the base bit/rate is doubled for PSK4 and multiplied by 4 for PSK8. Carrier frequency is 1.6 kHz and bandwidth's are variable depending on symbol rate. There is some doubts about the behaviour of the acoustic transducer in that frequency band since the transfer function is known only up to 1.1 Khz as shown in figure 5.2. Code names are madeup as follows: a maximum of 10 characters 'NiiPSKmbbb' where

ii	data stream duration in seconds	5 or 20
m	PSK modulation type	2,4 or 8
bbb	bit rate in bits/s; te=only 1's or lf=LFM's (no data)	75,150,300,te or lf

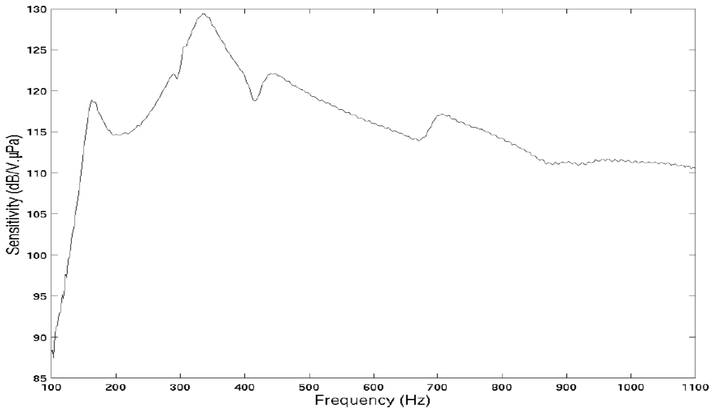

Figure 5.2: *HX90 acoustic source sensitivity*

5.1.4 Events 2 and 3: code A3

Acoustic transmissions during Events 2 and 3 always used code A3. Code A3 is a 2 s-duration linear-frequency-modulated (LFM) up-sweep with bandwidth 250 - 600 Hz. The repetition rate is 10 s, instead of the 8 s stated in the test plan, in order to allow a 20% duty cycle for the power amplifier to cool off. The transducer measured transfer function is shown in figure 5.2.

5.2 Received signals

The acoustic data was received on a 16-hydrophone, 4m-spacing VLA located at [008° 55' 55.8456" W - 38° 17' 56.7182" N]. The array mechanical structure is shown in figure 2.2. Taking as reference the depth recording at pressure gauge Pr1 the nominal depths for each hydrophone are given in Table 5.2.

From an electronic point of view one should note that there is a 180° phase shift between the top first 8 and the bottom 8 hydrophones as can be seen in figure 5.3. The signals received in the VLA are transmitted via an high speed RF link to onboard ship. At reception and prior to computer recording, signals are marked with a synchro top. That synchro top is obtained through GPS synchronization with the source emitted signal, thus absolute travel times can be computed from the received time series. Two of those synchro tops can also be seen in figure 5.3.

The pre-processing and analysis of the received signals is different for Events 1, and 2 and 3 and will be threfeore discussed separately for each case.

Table 5.2: *Hydrophone array depth*

Hyd. #	**Depth** (m)	**Hyd.** #	**Depth** (m)
1	32	9	64
2	36	10	68
3	40	11	72
4	44	12	76
5	48	13	80
6	52	14	84
7	56	15	88
8	60	16	92

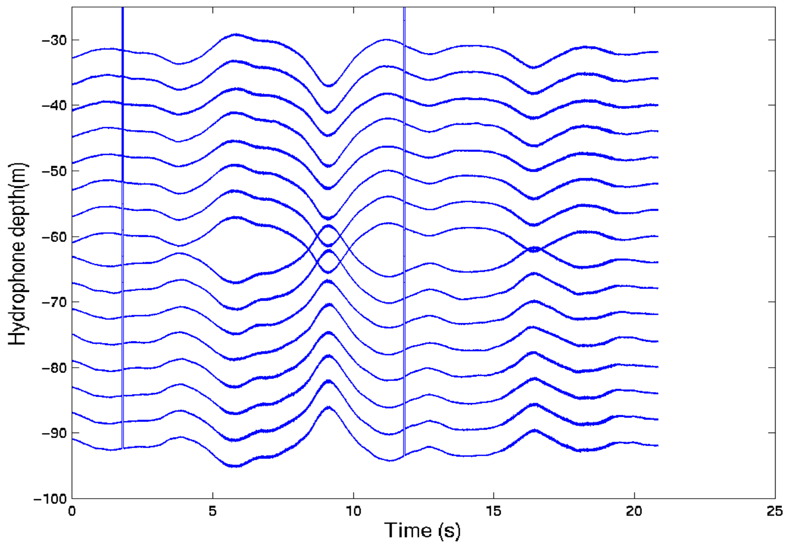

Figure 5.3: *Example of phase inversion between top 8 and bottom 8 hydrophones.*

5.3 Event 1: time-reversal mirror testing

For visualization purpose the signals of Event 1 have been bandpass filtered with a 5th order Buterworth digital filter centered on 1.6 kHz and a bandwidth of 800 Hz whose transfer function is shown in figure 5.4. As an example, the signals received at the top first 8 hydrophones of the VLA when code N20PSK275 is being transmitted are shown in figure 5.5.

One can easily see the mainlobe of the probe signal at approximately 0.75 s (0.25 s of propagation delay) and the 20 s long PSK2 modulated binary data sequence. Source - receiver range is approximately 350 m. For hydrophone 1, the time-frequency plane of a N20PSK275 code is shown in figure 5.6 where one can distinguish the probe signal and the data sequence with a bandwidth of roughly 100 Hz centered in 1600 Hz. Figure 5.7 shows a blowup of the first 2 seconds of the signal spectrogram where the probe signal can be now easily seen at approximately 0.75 seconds after signal transmission and then the start of the transmission of the data sequence at 1.2 s.

One of the most interesting features when using the Time-Reversal Mirror (TRM)

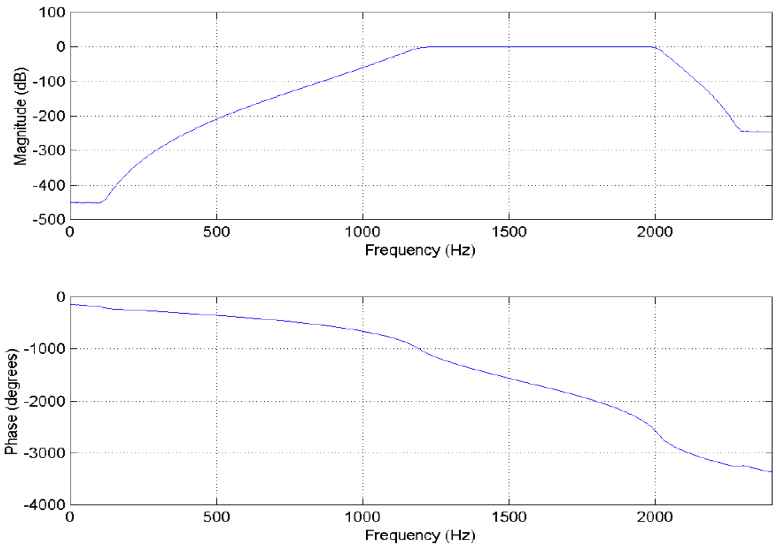

Figure 5.4: *Transfer function of bandpass filter used for visualization of received signals during Event 1.*

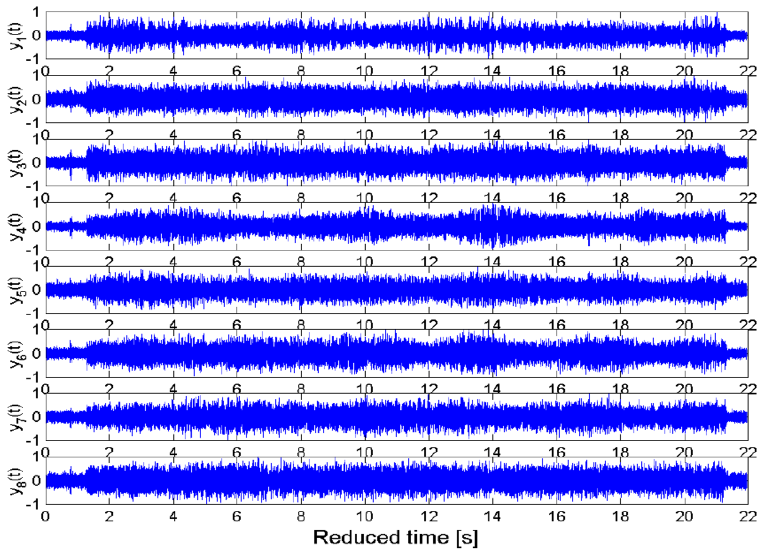

Figure 5.5: *Event 1: received code N20PSK275 for hydrophones 1 to 8.*

approach is the ability to extract the channel impulse response from the pulse shape for data filtering. The probe signal (PS) received on hydrophone 9 for a 75 bits/s data rate is shown in figure 5.8.

The root-root raised cosine pulse shape can be easily seen between 0.75 and 0.8 seconds, while the peaks at 0.81 and possibly at 0.86 are multipaths of the PS. If the emitted PS is used to pulse compress that time series one obtains the signal shown in figure 5.9. Note the main direct path at 0.77 s and the two surface and bottom paths respectively at 0.81 and 0.86 s. This pulse compressed signal is an estimate of the channel impulse response in that frequency band (approximately 100 Hz centered on 1.6 kHz) and for that source-receiver configuration. Whether that estimated channel impulse response is sufficiently

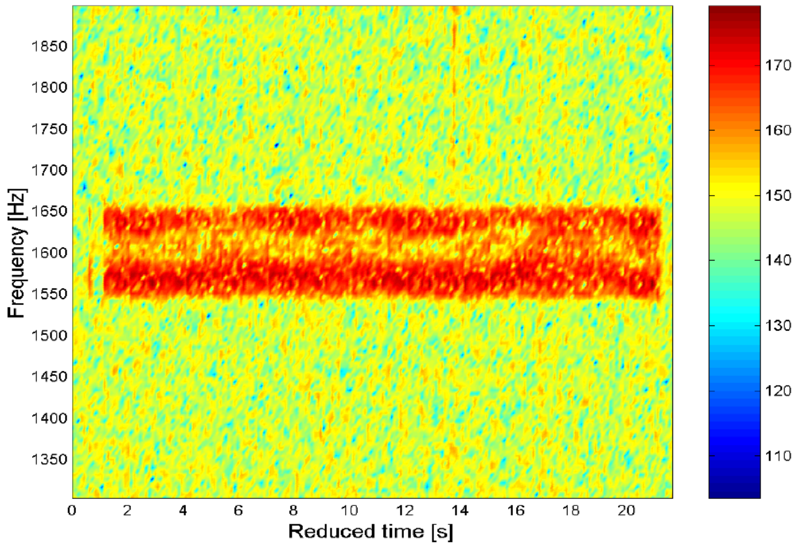

Figure 5.6: *Time-frequency plot of received code N20PSK275, at hydrophone 1 during Event 1.*

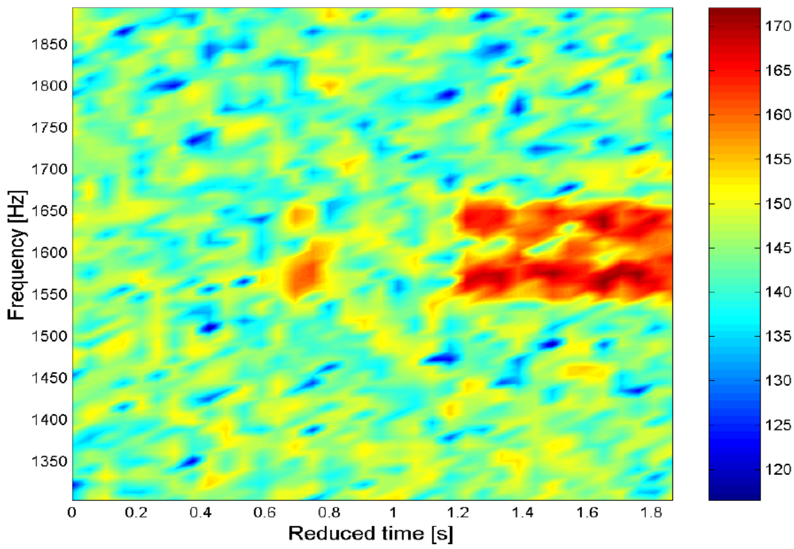

Figure 5.7: *Blowup of time-frequency plot of received code N20PSK275, at hydrophone 1 during Event 1: first 2 seconds.*

stable along time to deconvolve the data sequence following the probe signal is a main issue to be demonstrated in a future detailed data analysis of Event 1. In the sequel the pulse compression of the probe signal of each code being transmitted will be used as a qualitative measure of quality of the communication channel.

In order to demonstrate the spatial variability of the channel impulse response at those frequencies, figure 5.10 shows the pulse compressed estimated impulse response along the VLA for all the 16 hydrophones with number 1 being the shallowest hydrophone at about 30 m depth. Impulse reponses are normalized and aligned on the emitted signal synchro top.

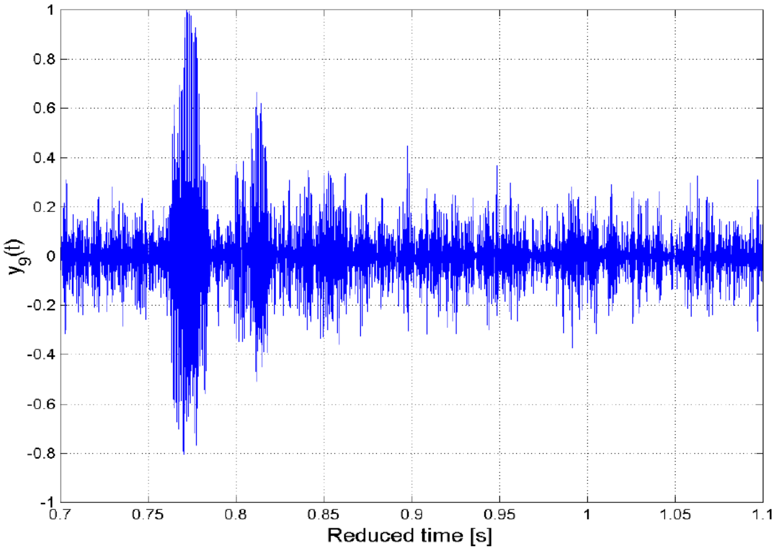

Figure 5.8: *Received probe signal on hydrophone 9 for the 75 bits/s data rate.*

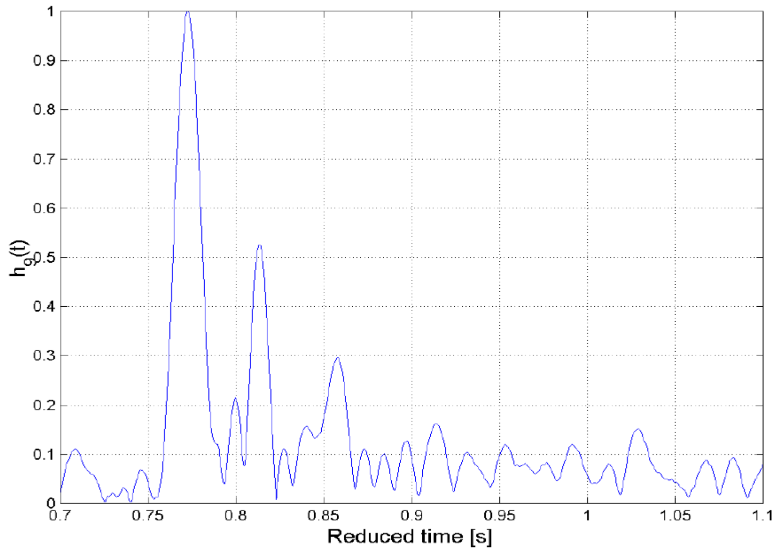

Figure 5.9: *Pulse compressed received probe signal on hydrophone 9 for the 75 bits/s data rate.*

Figure 5.11 shows the pulse compressed plot of the estimated channel impulse response for all the signals received at station 1 at an approximate source receiver range between 300 and 600 m. White lines are periods where the acoustic source was shut off for changing code. Synchronization was made on the transmitted signal synchro top, therefore the arrivals are not self aligned and the change in arrival time denotes ship drifting during the station. The code sequence is given in table 5.3. There are only 20 codes while 22 were transmitted: the missing received signals were largely perturbated by RF transmission between the radio buoy and the ship and therefore eliminated from the plot.

As observing the sucessive channel estimates along station 1 several remarks can be made: at each sequence of 75, 150 and 300 symbol rate, clear differences between band-

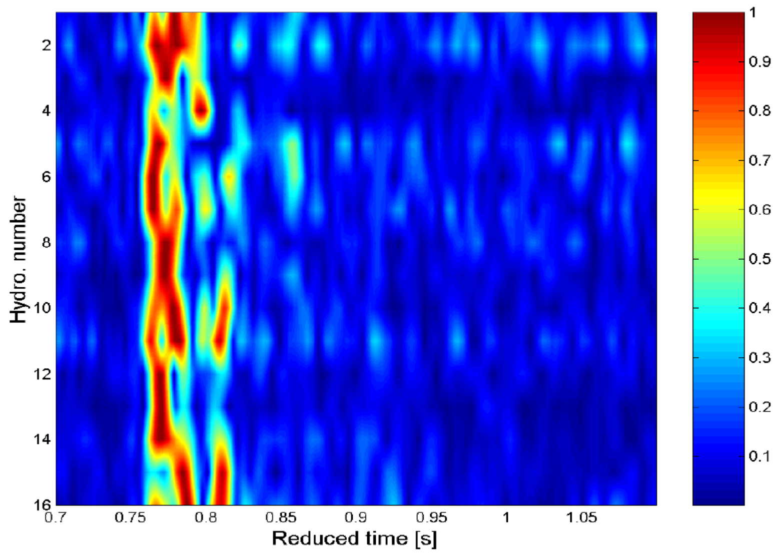

Figure 5.10: *Pulse compressed received probe signal for all hydrophones and for the 75 bits/s data rate.*

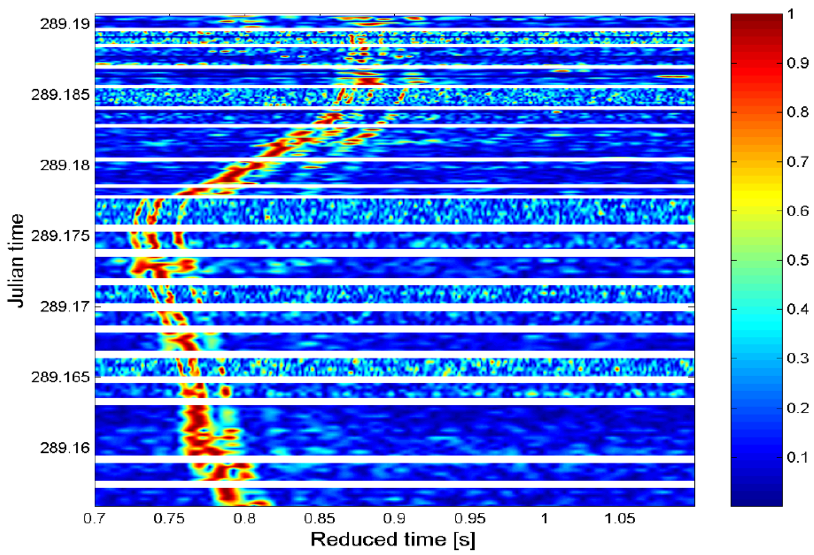

Figure 5.11: *Pulse compressed received probe signal for hydrophone 1 and all codes during station 1.*

widths can be noticed; path resolution is higher for the higher symbol rates, i.e., the larger bandwidth, where three strong paths can be clearly seen; that higher resolution also contributes to peek up very low energy paths along the impulse response time window.

Figure 5.12 shows the pulse compressed estimated channel impulse response for codes N20PSK4150 (bottom) and N20PSK2300 (top) during course between station 1 and station 2. It can be remarked that although no precise impulse response evolution can be seen along time a main peak can be followed as the source-receiver range increases. This can be easily seen for the bottom figure at 150 symb/s but not for the larger frequency band at 300 symb/s (top). It should be pointed out that this base band processing is

Table 5.3: *Event 1: transmitted code sequence.*

Code	**Probe**		**Data**		**Symb.rate**	**BW**	**Rep.rate**
	Type	duration (s)	Type	duration (s)	(symb/s)	(Hz)	(s)
N20PSK2te	PS75	1	PSK2	20		112.5	22
N20PSK2lf	PS75	10	LFM	10		112.5/800	22
N20PSK275	PS75	1	PSK2	20	75	112.5	22
N20PSK2150	PS150	1	PSK2	20	150	225	22
N20PSK2300	PS300	1	PSK2	20	300	450	22
N20PSK475	PS75	1	PSK4	20	150	112.5	22
N20PSK4150	PS150	1	PSK4	20	300	225	22
N20PSK4300	PS300	1	PSK4	20	600	450	22
N20PSK875	PS75	1	PSK8	20	300	112.5	22
N20PSK8150	PS150	1	PSK8	20	600	225	22
N20PSK8300	PS300	1	PSK8	20	1200	450	22
N5PSK2te	PS75	1	PSK2	5		112.5	7
N5PSK2lf	PS75	3	LFM	3		112.5/800	7
N5PSK275	PS75	1	PSK2	5	75	112.5	7
N5PSK2150	PS150	1	PSK2	5	150	225	7
N5PSK2300	PS300	1	PSK2	5	300	450	7
N5PSK475	PS75	1	PSK4	5	150	112.5	7
N5PSK4150	PS150	1	PSK4	5	300	225	7
N5PSK4300	PS300	1	PSK4	5	600	450	7
N5PSK875	PS75	1	PSK8	5	300	112.5	7
N5PSK8150	PS150	1	PSK8	5	600	225	7
N5PSK8300	PS300	1	PSK8	5	1200	450	7

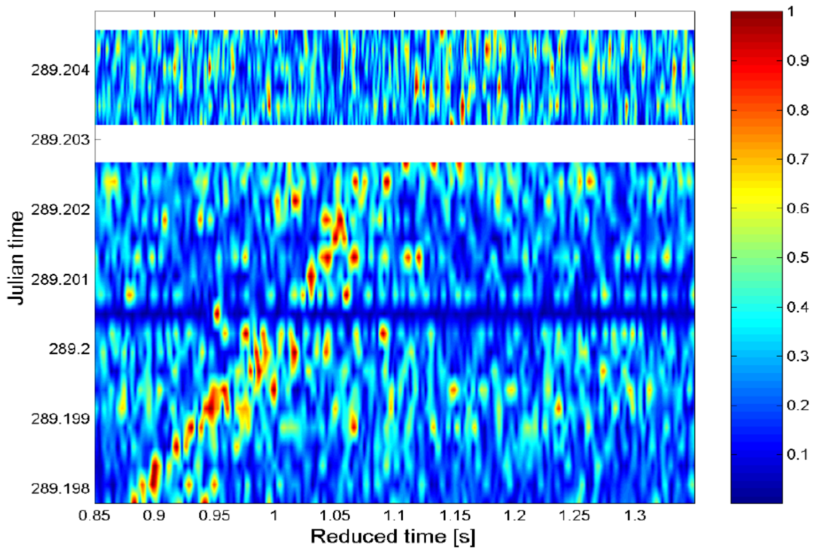

Figure 5.12: *Pulse compressed received probe signal for hydrophone 1 and all codes during the course between station 1 and station 2.*

made without any Doppler compensation which is particularly severe when the source is moving and at higher frequencies.

The results shown in figure 5.13 are relative to the pulse compression of the signals received on hydrophone 1 during station 2 at approximately 1.2 km source-receiver range. The code sequence is the same as that for station 1 and given in table 5.3. Comparing these results it can be seen that the number of paths has clearly increased due to the larger range.

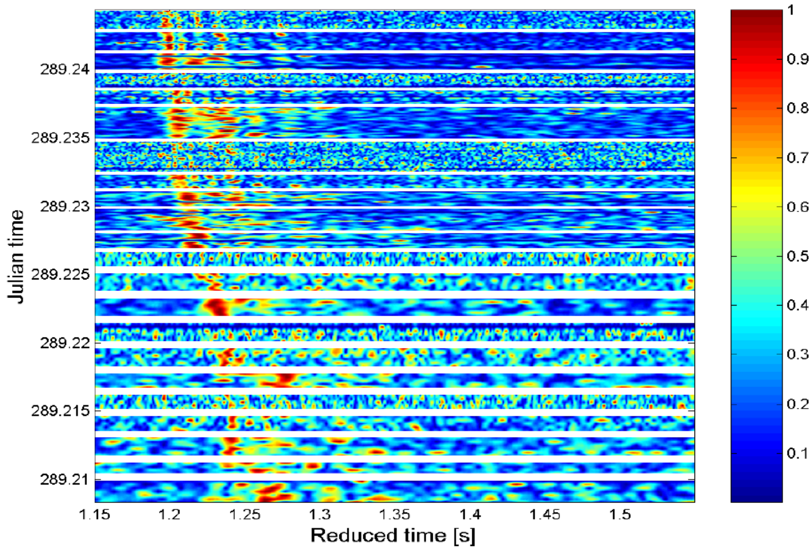

Figure 5.13: *Pulse compressed received probe signal for hydrophone 1 and all codes during station 2.*

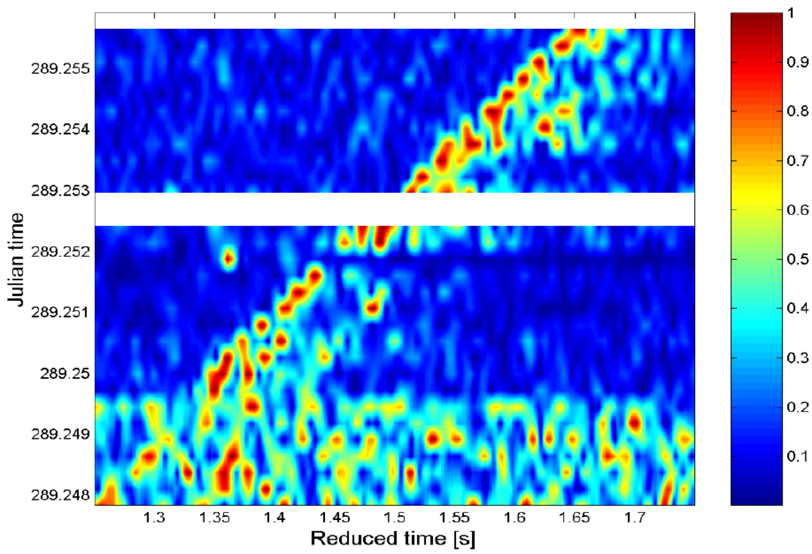

Figure 5.14: *Pulse compressed received probe signal for hydrophone 1 and all codes during part of the course between station 2 and station 3.*

Figures 5.14 and 5.15 show the estimated impulse responses from the signals received on hydrophone 1 during the transect from station 2 to station 3. The first part of figure 5.14

corresponds to the transmission of test code N20PSK2te where no clear channel response could be seen. The remaining part of figure 5.14 (before and after the source interruption at 289.2525) has been obtained with code N20PSK275 where double or triple multipath can be seen.

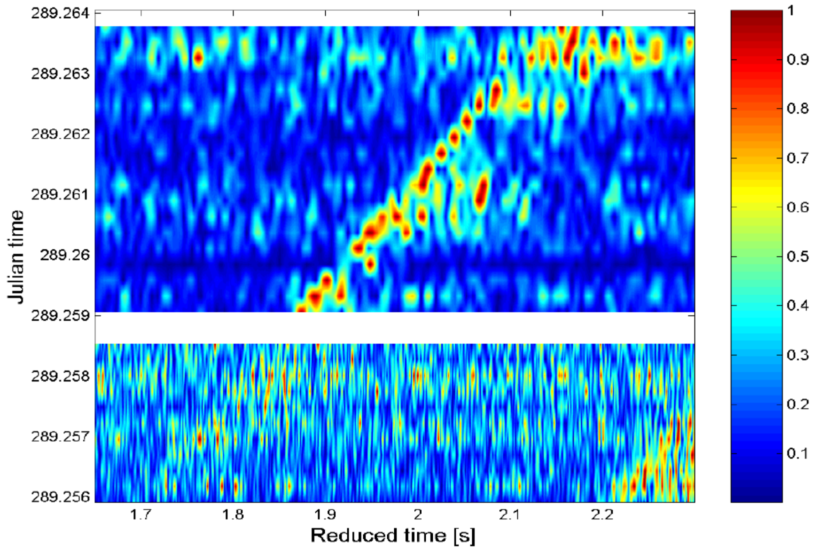

Figure 5.15: *Pulse compressed received probe signal for hydrophone 1 and all codes during part of the course between station 2 and station 3.*

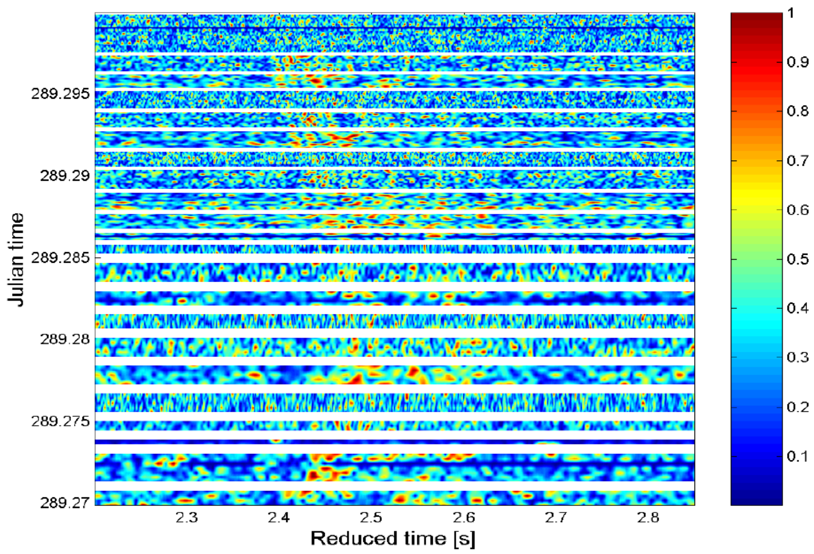

Figure 5.16: *Pulse compressed received probe signal for hydrophone 1 and all codes during station 3.*

Figure 5.15 shows two distinct parts for transmitted coded N20PSK2300(bottom) and N20PSK475 (top). The strong arrivals on the right side of the lower part of the bottom transmission are simply due to a spectral overlap due to the larger band of the signal relative to the top signal. As previsouly no Doppler compensation has been used in this processing Figure 5.16 shows the pulse compressed results obtained from the signals received at hydrophone 1 during station 3 at approximately 3 km from the source and for all codes of table 5.3. Impulse response estimation is clearly very noisy due to the low signal to noise ratio at such long range and for the given source power.

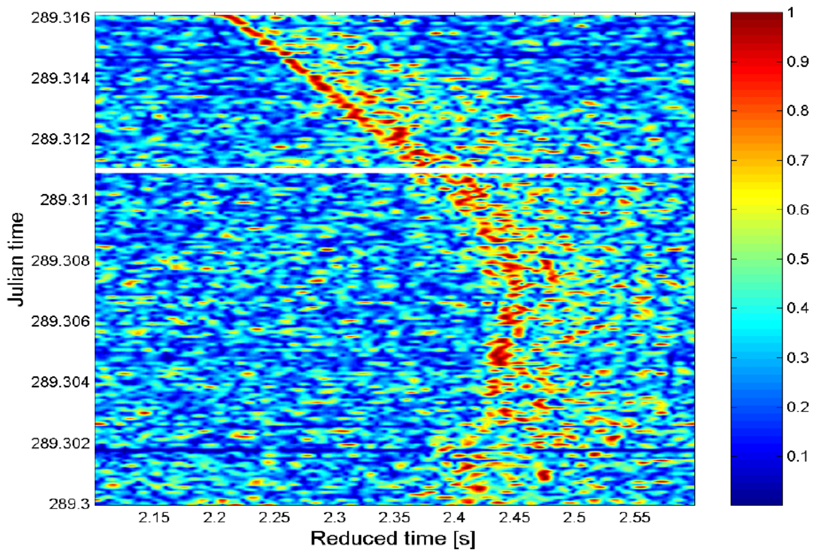

Figure 5.17: *Pulse compressed received probe signal for hydrophone 1 and all codes during part of the course between station 3 and station 4.*

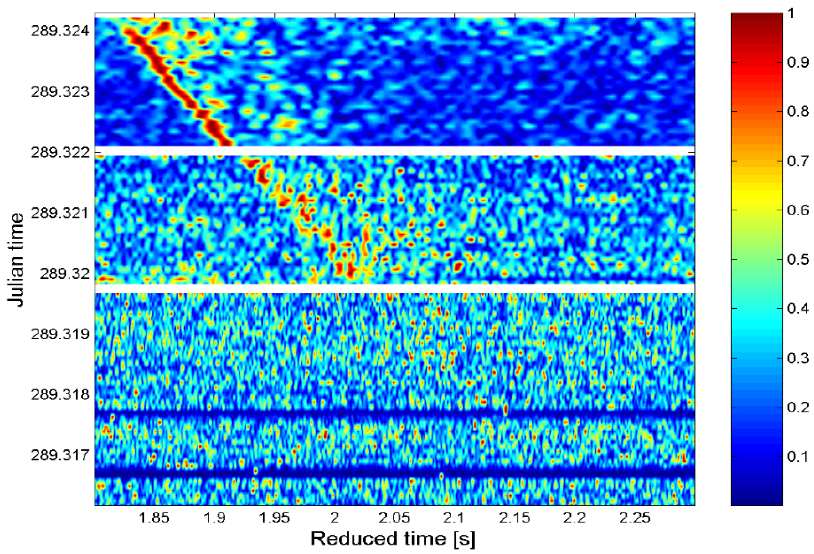

Figure 5.18: *Pulse compressed received probe signal for hydrophone 1 and all codes during part of the course between station 3 and station 4.*

During the transect from station 3 to station 4, closing range to the VLA, the transmitted codes where N5PSK2te (twice) (figure 5.17) and N5PSK2300, N5PSK2150 and N20PSK275 as shown in figure 5.18. The source closing range path can be easily followed with a clear decrease of multipath extent while the signal is completely lost during the code N5PSK2300 and recovered for the last two codes.

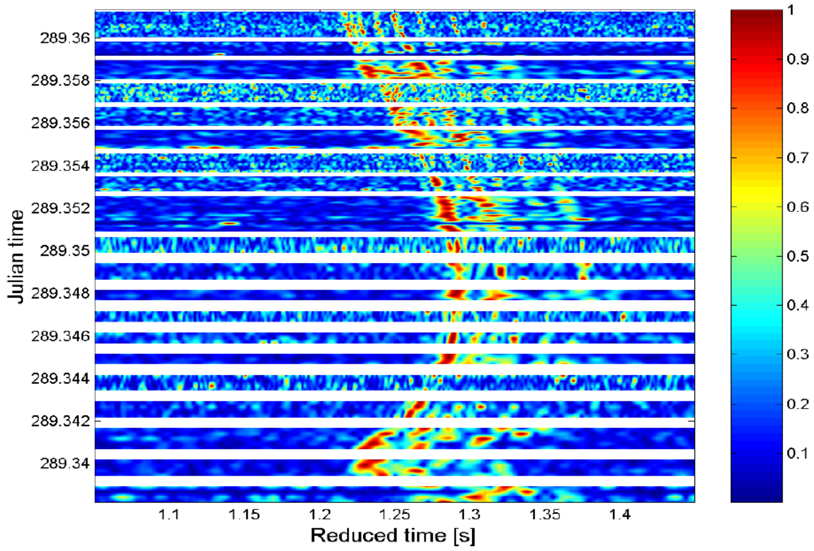

Figure 5.19: *Pulse compressed received probe signal for hydrophone 1 and all codes during station 4.*

Finally, the pulse compression of the signals received on hydrophone 1 during the last station at approximately the same location as station 1 are shown in figure 5.19. Again the code sequence is that given in table 5.3 with the exception of codes N5PSK2te and N5PSK2lf that were not transmitted in that last station.

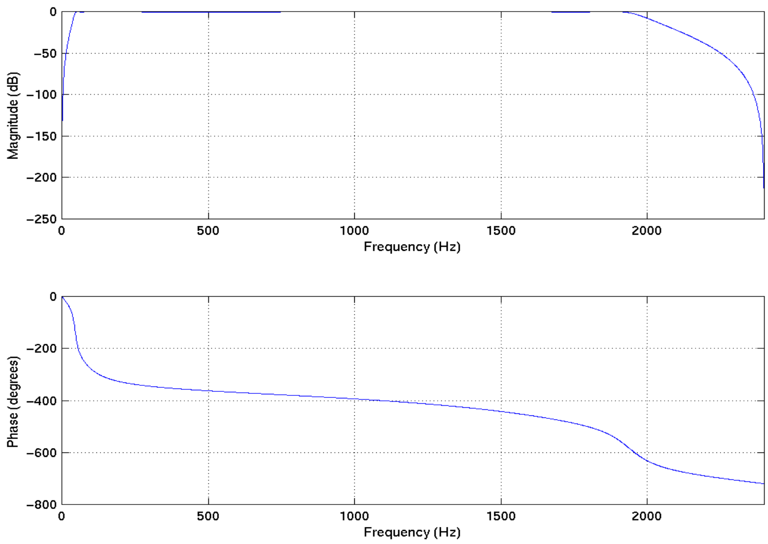

Figure 5.20: *Chebychev 4th-order [48,1920] Hz, band-pass filter amplitude frequency response.*

5.4 Event 2: range independent acoustic transmissions

The signals received during Event 2 were pre-processed prior to visualization. The pre-processing has two stages: first, the synchro top signals are detected and then eliminated and second, the low frequency high amplitude signal components due to current flow (figure 5.3) are filtered.

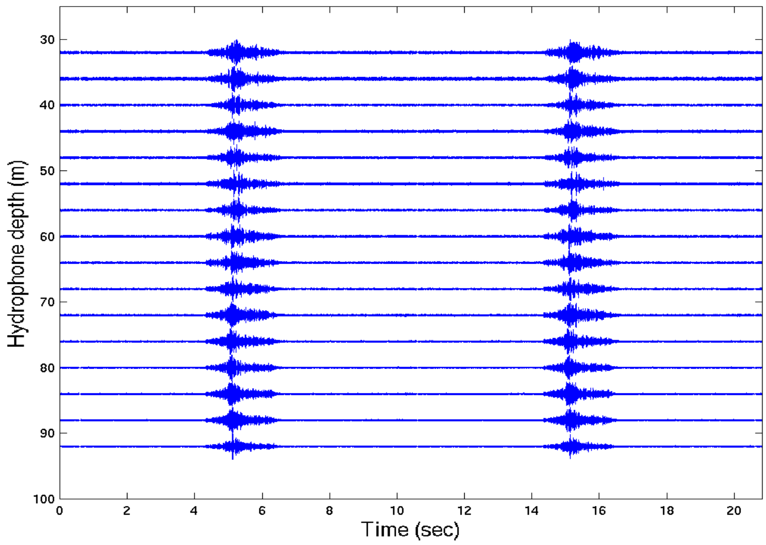

Figure 5.21: *Received signals during Event 2 after pre-processing.*

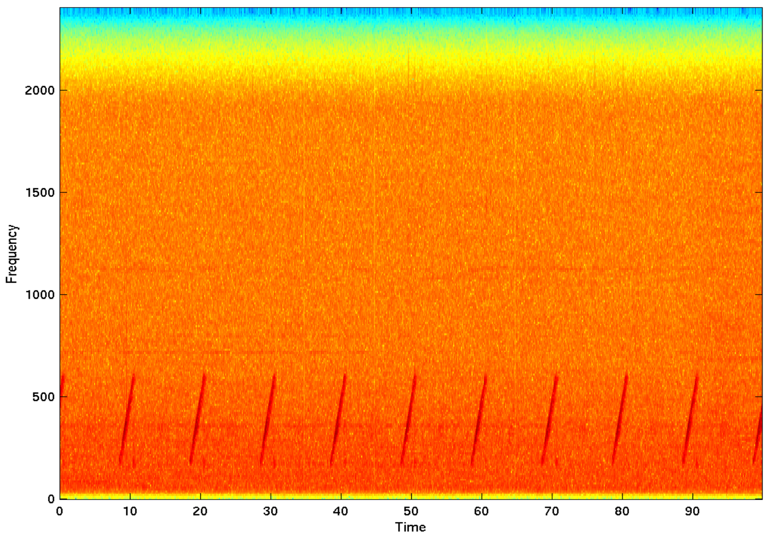

Figure 5.22: *Event 2: spectrogram of the signal received on hydrophone 8.*

The first step is easily accomplished with a peak detector. The second step consists in passing the received signals through a band-pass filter to eliminate the undesired frequency components. This is performed by a 4th-order Chebychev digital band-pass filter in the band [48,1920] Hz, which modulus frequency response is given in figure 5.20.

As an example figure 5.21 shows the signals after pre-processing received at all hydrophones during Event 2. The spectrogram (short Fourier transform) of the received signal at hydrophone 8 for a series of snapshots can be seen in figure 5.22. As a measure the stability of the acoustic channel it is common to pulse compress the received signal with the transmitted pulse (matched filtering). The result obtained during Event 2 and for hydrophone 8 is shown in figures 5.23 and 5.24 with the alignement made on the synchro pulse and auto-aligned (leading pulse) respectively.

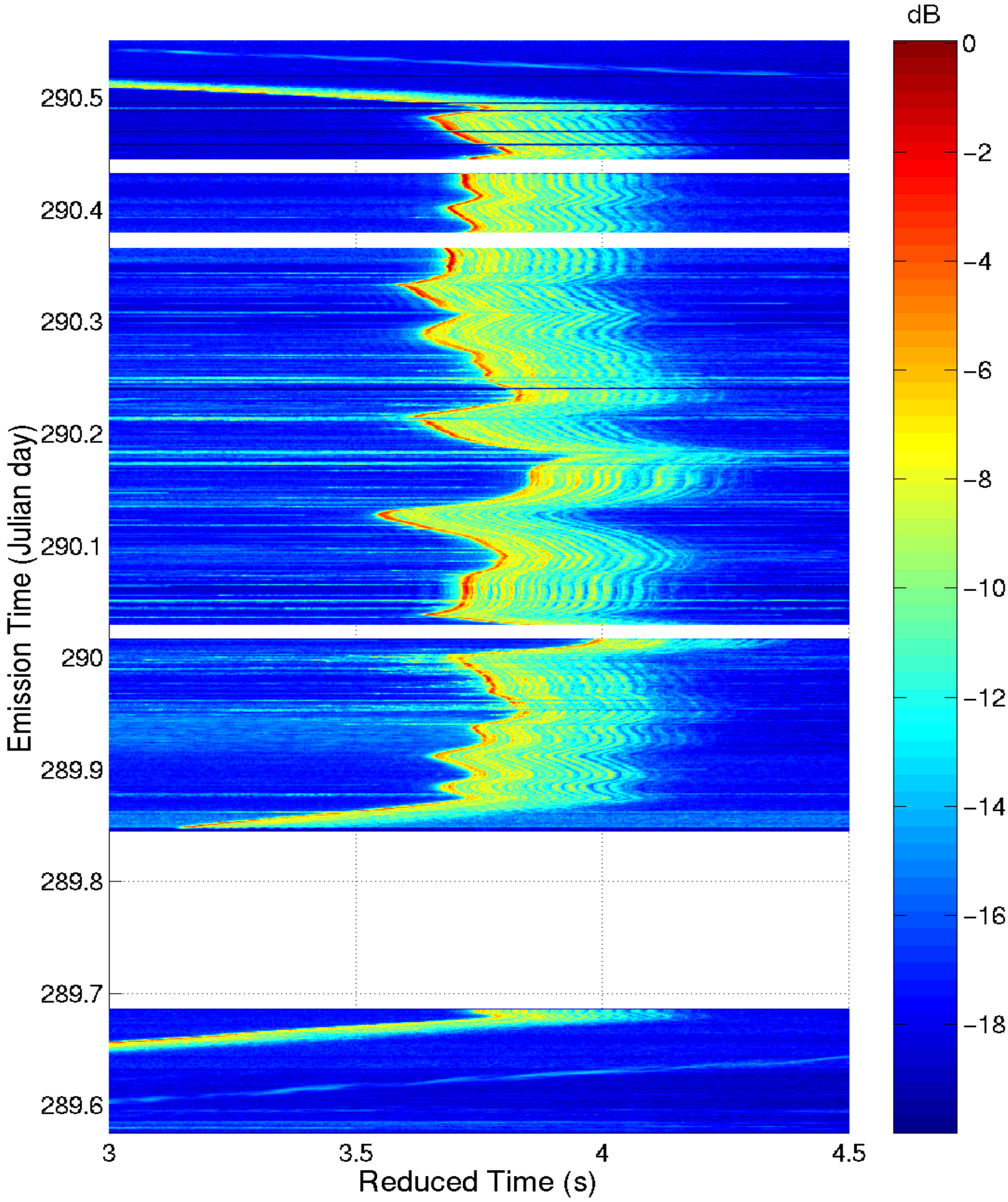

Figure 5.23: *Pulse compressed arrival patterns during Event 2 with synchronization on the emitted signal .*

The source aligned arrival pattern shows that the source ship had an important drift during transmissions with the source-receiver range varying up to 400 m in 5.2 km. This

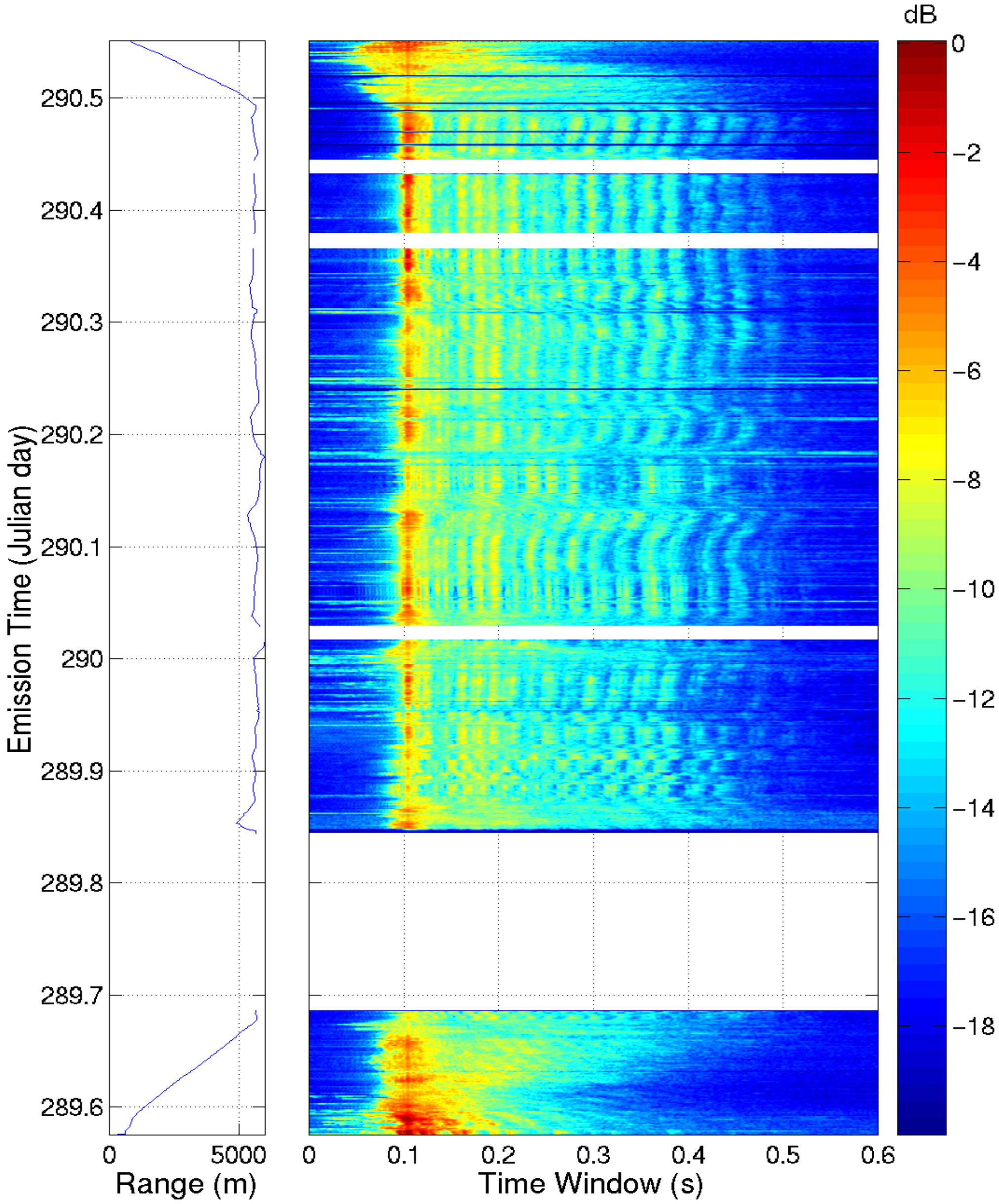

Figure 5.24: *Pulse compressed arrival patterns during Event 2 with leading edge synchronization (right) and estimated source-VLA range (left).*

type of synchronization may allow for estimating absolute travel times and possibly employ classical ray-based tomographic inversion. The right plot in figure 5.24 shows a very stable arrival pattern with arrivals separated in up to 12 resolved packets. Clear oscillations in the late arrivals may denote some internal wave activity, to be correlated or validated with temperature and/or current data. In both figures, amplitudes have been normalized by the strongest arrival.

5.5 Event 3: across canyon acoustic transmissions.

The pre-processing is identical to that of Event 2. The received time series on all hydrophones is shown in figure 5.25. Compared with the time series obtained for Event 2, there is more interference noise that might be due to particular conditions at the VLA. In particular, hydrophone 9 seems to be quite noisy in this recording.

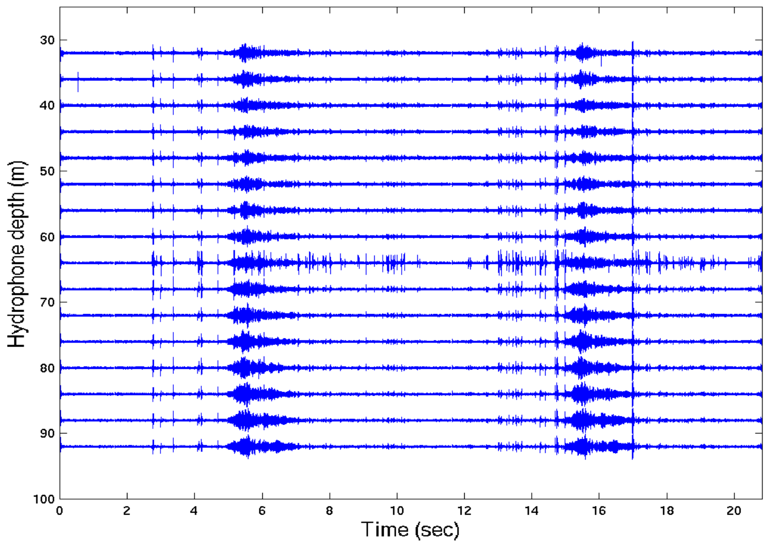

Figure 5.25: *Received signals during Event 3.*

The spectrogram of the signal received in hydrophone 8 for a series of snapshots can be seen in figure 5.26.

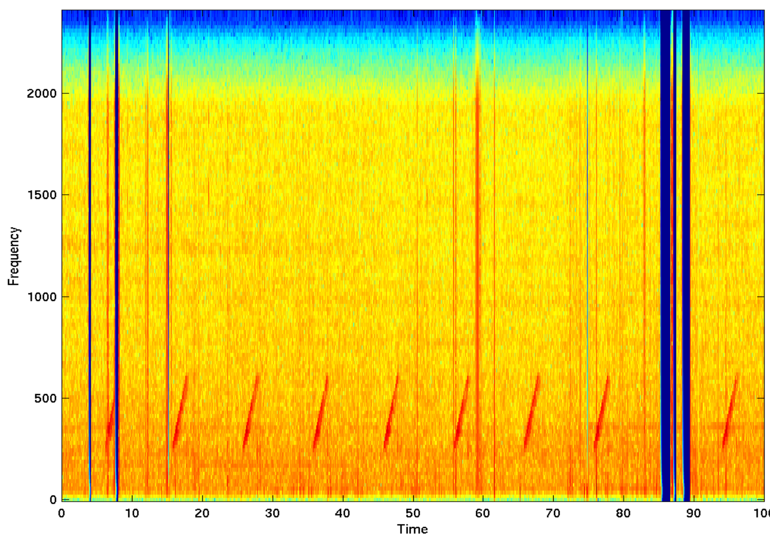

Figure 5.26: *Event 3: spectrogram of the signal received on hydrophone 8.*

The pulse-compression results for hydrophone 8 obtained during Event 3 are shown in figures 5.27 and 5.28 for synchro top signal aligned and leading edge signal aligned arrival patterns, respectively. The arrival pattern is not so clearly resolved in this data as in that of Event 2. One remarquable fact is the strong attenuation of the received pattern during certain short periods of time, as for example, at 291.65 and between 291.98 and 291.20.

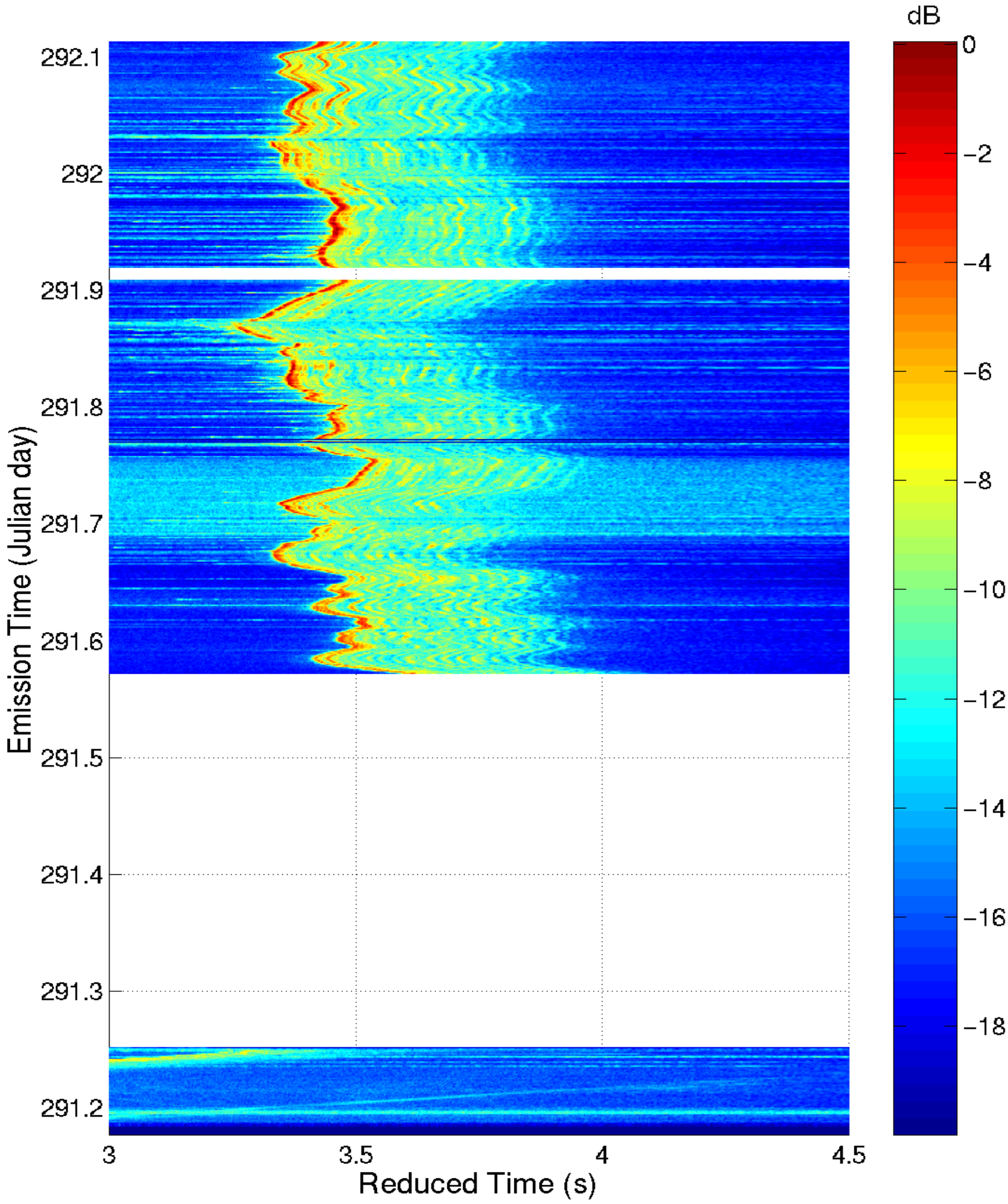

Figure 5.27: *Pulse compressed arrival patterns during Event 3 with synchronization on the emitted signal (hydrophone 8).*

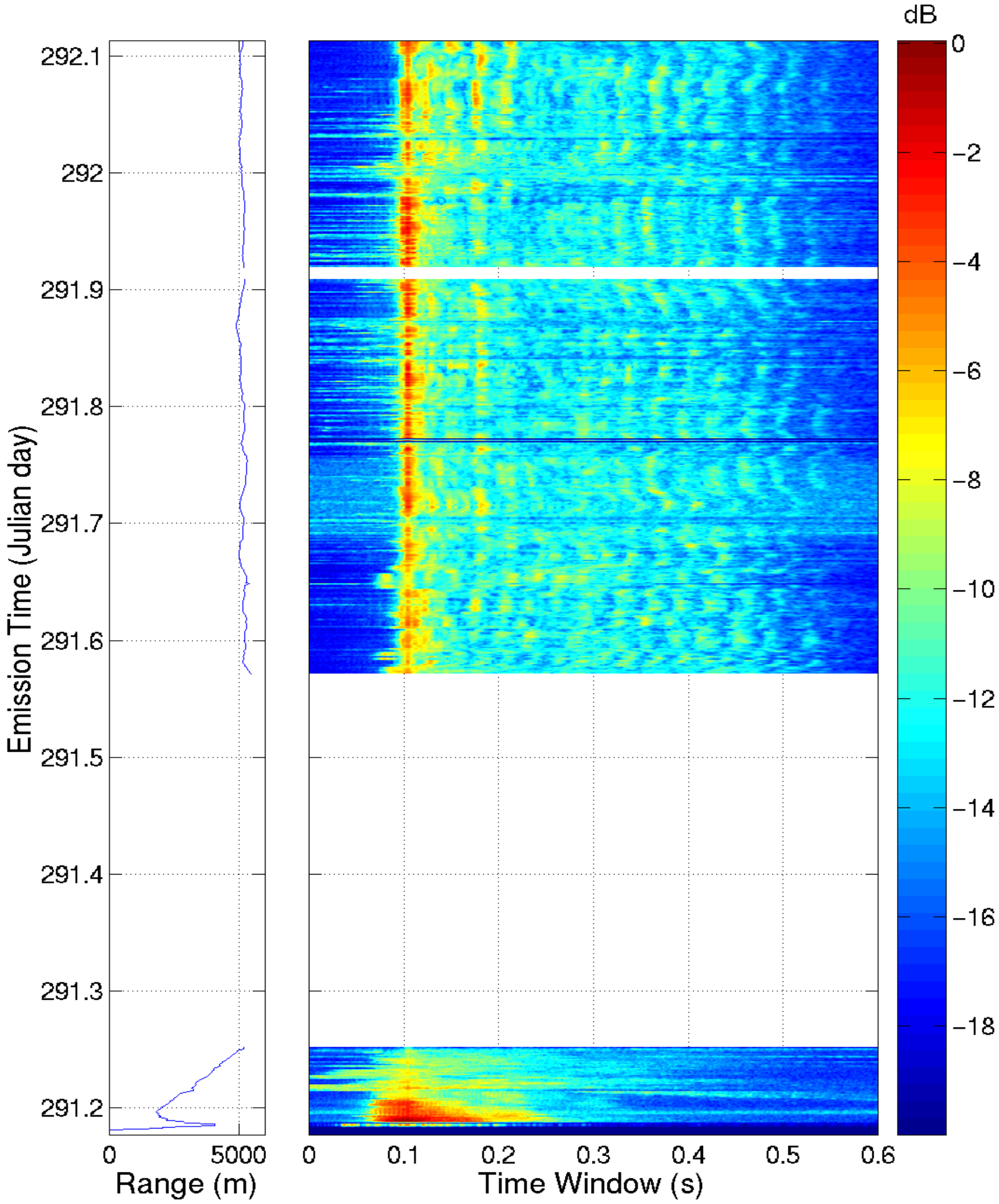

Figure 5.28: *Pulse compressed arrival patterns during Event 3 with leading edge synchronization (right) and estimated source-VLA range (left) (hydrophone 8).*

Chapter 6

Conclusion

INTIFANTE'00 was an ambitious sea trial that covered a very broad number of aspects from tomography to source localization and from underwater communications to remote navigation. The present work reports the data gathered to support part of the underwater communications effort, project INFANTE, and the tomography and source localization efforts under the ending project INTIMATE, to be continued under ATOMS.

Under the underwater communications effort, the objective was to test the capabilities of the time-reversal mirror technique at low frequency and at low data rates. With the limitations imposed by the acoustic source that was not garanteed for the required bandwidth, we believe that a good data set has been acquired and its processing is underway.

The internal tide tomography is now a classic objective for CINTAL and IH teams that are exploiting their third set of real data. The data set acquired during Event 2 is very much alike that of the phase 1 of the INTIMATE'96 sea trial with however a few differences: the period of the year and the geographic position of the submarine canyon relative to the acoustic test site. From the technical point of view also, the acoustic receiving array was now much more populated (16 hydrophones) than that used in 1996 (4 hydrophones, 3 working). The acoustic transmissions across the submarine canyon made during Event 3, represent a real challenge for acoustic modeling both for tomographic inversion and source localization purposes. The acoustic signals recorded during that event seem to have a higher variability and to be much less resolved in the classicaly stable late arrivals, which are those generally used for data inversion.

The acoustic data inversion results are to be validated by the environmental data recorded *in situ* during the experiment. This data comprises water column temperature profiles, both at the acoustic array location and at the source position (XBT's) and bathymetry tracks. Geoacoustic information will be provided in the companion IH INTIFANTE'00 data report. Finally source-receiver geometry in terms of hydrophone array position, ship course and source depth completes this data set.

Bibliography

[1] W. Munk and C. Wunsch, “Ocean Acoustic Tomography: a scheme for large scale monitoring”, Deep-Sea Research, Vol. 26A, pp. 123-161, 1979.

[2] W. Munk, P. Worcester and C. Wunsch, *Ocean Acoustic Tomography*, Cambridge Monographs on Mechanics, New York, USA, 1995.

[3] S.M.Jesus, “Tomografia Passiva Costiera, Data Report - Phase 1”, SiPLAB Rep 01/01, March 2001.

[4] ”INTIFANTE’00 Test Plan”, INTIMATE Group, October 2000.

[5] Small J. and Dovey P., “INTIFANTE 99 Oceanographic Data Report”, DERA Report DERA/S&P/UWS/WP990213, November 1999.

[6] BEJA J., ”Relatório de de progresso de trabalhos - INTIFANTE’99”, REL TP OC 02/00, Instituto Hidrográfico, Lisboa, March 2000.

Appendix A

INTIFANTE'00 CD-ROM list

Table A.1 lists all CD-ROM's containing the acoustic and non-acoustic data sets for Events 1, 2 and 3.

Table A.1: *CD-ROM list: events 1,2 and 3.*

Event#	**CD**	Run	Snapshot	Time
1	INT00-0001	1	01-21	03:34:25
	INT00-0002	1	22-42	04:09:25
	INT00-0003	1	43-63	04:44:49
	INT00-0004	1	64-84	05:20:03
	INT00-0005	1	85-105	05:55:13
	INT00-0006	1	106-126	06:30:11
	INT00-0007	1	127-147	07:05:15
	INT00-0008	1	148-168	07:40:18
	INT00-0009	1	169-184	08:15:15
2	INT00-0010	1	01-21	13:48:18
	INT00-0011	1	22-42	14:23:31
	INT00-0012	1	43-63	14:58:35
	INT00-0013	1	64-84	15:33:36
	INT00-0014	1	85-97	16:08:32
		2	01-09	20:16:02
	INT00-0015	2	10-30	20:31:00
	INT00-0016	2	31-51	21:06:15
	INT00-0017	2	52-72	21:41:11
	INT00-0018	2	73-93	22:16:12
	INT00-0019	2	94-114	22:51:17
	INT00-0020	2	115-135	23:27:05
	INT00-0021	2	136-149	00:02:25
		3	01-08	00:41:41
	INT00-0022	3	09-29	00:55:12
	INT00-0023	3	30-50	01:30:23
	INT00-0024	3	51-71	02:05:34
	INT00-0025	3	72-92	02:40:37

Table A.2: *CD-ROM list: events 1,2 and 3 (cont.)*

Event#	**CD**	Run	Snapshot	Time
	INT00-0026	3	93-113	03:15:42
	INT00-0027	3	114-134	03:50:46
	INT00-0028	3	135-155	04:27:02
	INT00-0029	3	156-176	05:02:04
	INT00-0030	3	177-197	05:37:58
	INT00-0032	3	198-218	06:14:00
	INT00-0032	3	219-239	06:49:03
	INT00-0033	3	240-260	07:24:06
	INT00-0034	3	261-281	07:59:17
	INT00-0035	3	282-289	08:34:36
		5	01-13	09:06:27
	INT00-0036	5	14-34	09:28:10
	INT00-0037	5	35-47	10:03:06
		6	01-09	10:39:57
	INT00-0038	6	10-30	10:55:04
	INT00-0039	6	31-51	11:30:09
	INT00-0040	6	52-72	12:05:15
	INT00-0041	6	73-93	12:40:15
3	INT00-0042	1	01-21	04:14:24
	INT00-0043	1	22-42	04:49:22
	INT00-0044	1	43-63	05:24:22
	INT00-0045	1	64-65	06:00:06
		2	01-20	13:42:18
	INT00-0046	2	21-41	14:15:34
	INT00-0047	2	42-62	14:51:23
	INT00-0048	2	63-83	15:26:53
	INT00-0049	2	84-104	16:02:40
	INT00-0050	2	105-125	16:40:02
	INT00-0051	2	126-146	17:17:38
	INT00-0052	2	147-167	17:52:45
	INT00-0053	2	168-188	18:28:51
	INT00-0054	2	189-209	19:04:53
	INT00-0055	2	210-230	19:41:30
	INT00-0056	2	231-251	20:19:11
	INT00-0057	2	252-259	20:56:55
	INT00-0058	3	01-22	21:12:34

Table A.3: *CD-ROM list: events 1,2 and 3 (cont.)*

Event#	**CD**	Run	Snapshot	Time
	INT00-0059	4	01-21	22:03:32
	INT00-0060	4	22-42	22:38:53
	INT00-0061	4	43-63	23:14:44
	INT00-0062	4	64-84	23:52:26
	INT00-0063	4	85-105	00:28:28
	INT00-0064	4	106-126	01:06:47
	INT00-0065	4	127-147	01:42:24
	INT00-0066	4	148-164	02:17:40
Non-acoustic	INT00-0086	-	–	—-
	INT00-0087	-	–	—-
	INT00-0088	-	–	—-

Appendix B

Code list for Event 1

Table B.1 lists all codes transmitted at the different stations during Event 1.

Table B.1: *Event 1 PSK-code list*

Code	Start time (GMT)	Station
N20PSK2te	03:46:00	S1
N20PSK2lf		
N20PSK275		
N20PSK2150		
N20PSK2300		
N20PSK475		
N20PSK4150		
N20PSK4300		
N20PSK875		
N20PSK8150		
N20PSK8300		
N5PSK2te	04:20:00	
N5PSK2lf		
N5PSK275		
N5PSK2150		
N5PSK2300		
N5PSK475		
N5PSK4150		
N5PSK4300		
N5PSK875		
N5PSK8150		
N5PSK8300		

Table B.2: *Event 1 PSK-code list(cont.)*

Code	Start time (GMT)	Station
N20PSK24150		S1 to S2
N20PSK2300		
N20PSK2te	05:00:00	S2
N20PSK2lf		
N20PSK275		
N20PSK2150		
N20PSK2300		
N20PSK475		
N20PSK4150		
N20PSK4300		
N20PSK875		
N20PSK8150		
N20PSK8300		
N5PSK2te	05:30:00	
N5PSK2lf		
N5PSK275		
N5PSK2150		
N5PSK2300		
N5PSK475		
N5PSK4150		
N5PSK4300		
N5PSK875		
N5PSK8150		
N5PSK8300		
N20PSK2te		S2 to S3
N20PSK275		
N5PSK2300		
N5PSK475		
N20PSK2te	06:29:00	S3
N20PSK2lf		
N20PSK275		
N20PSK2150		
N20PSK2300		
N20PSK475		
N20PSK4150		
N20PSK4300		
N20PSK875		
N20PSK8150		
N20PSK8300		

Table B.3: *Event 1 PSK-code list (cont.)*

Code	Start time (GMT)	Station
N5PSK2te	06:55:00	
N5PSK2lf		
N5PSK275		
N5PSK2150		
N5PSK2300		
N5PSK475		
N5PSK4150		
N5PSK4300		
N5PSK875		
N5PSK8150		
N5PSK8300		
N5PSK2te		S3 to S4
N5PSK2300		
N5PSK2150		
N5PSK275		
N5PSK2te		
N5PSK2lf		
N5PSK2te		
N5PSK2lf		
N20PSK2te	08:07:00	S4
N20PSK2lf		
N20PSK275		
N20PSK2150		
N20PSK2300		
N20PSK475		
N20PSK4150		
N20PSK4300		
N20PSK875		
N20PSK8150		
N20PSK8300		
N5PSK2lf	08:27:00	
N5PSK275		
N5PSK2150		
N5PSK2300		
N5PSK475		
N5PSK4150		
N5PSK4300		
N5PSK875		
N5PSK8150		
N5PSK8300		
N5PSK2lf		